Neurobiology of Disease 138 (2020) 104789

Contents lists available at ScienceDirect

Neurobiology of Disease

journal homepage: www.elsevier.com/locate/ynbdi

Alpha-synuclein/synapsin III pathological interplay boosts the motor response to methylphenidate

Gaia Faustini[a], Francesca Longhena[a], Agostino Bruno[b], Federica Bono[a,c], Jessica Grigoletto[a], Luca La Via[d], Alessandro Barbon[d], Andrea Casiraghi[e], Valentina Straniero[e], Ermanno Valoti[e], Gabriele Costantino[b], Fabio Benfenati[f,g], Cristina Missale[a], Marina Pizzi[a], Maria Grazia Spillantini[h], Arianna Bellucci[a,c,*]

[a] Division of Pharmacology, Department of Molecular and Translational Medicine, University of Brescia, Viale Europa 11, 25123 Brescia, Italy
[b] Department of Food and Drug, University of Parma, Parco Area delle Scienze, 27/A, 43124 Parma, Italy
[c] Laboratory for Preventive and Personalized Medicine, Department of Molecular and Translational Medicine, University of Brescia, Viale Europa 11, 25123 Brescia, Italy
[d] Division of Biology and Genetics, Department of Molecular and Translational Medicine, University of Brescia, Viale Europa 11, 25123 Brescia, Italy
[e] Department of Pharmaceutical Sciences, University of Milan, Via Giuseppe Colombo 60, Milano, Italy
[f] Italian Institute of Technology, Via Morego 30, Genova, Italy
[g] IRCSS Policlinico San Martino Hospital, Largo Rosanna Benzi 10, 16132 Genova, Italy
[h] Department of Clinical Neurosciences, Clifford Albutt Building, University of Cambridge, Cambridge CB2 0AH, UK

ARTICLE INFO

Keywords:
Parkinson's disease
α-Synuclein
Synapsin III
Methylphenidate
Cocaine
Motor behaviour

ABSTRACT

Loss of dopaminergic nigrostriatal neurons and fibrillary α-synuclein (α-syn) aggregation in Lewy bodies (LB) characterize Parkinson's disease (PD). We recently found that Synapsin III (Syn III), a phosphoprotein regulating dopamine (DA) release with α-syn, is another key component of LB fibrils in the brain of PD patients and acts as a crucial mediator of α-syn aggregation and toxicity.

Methylphenidate (MPH), a monoamine reuptake inhibitor (MRI) efficiently counteracting freezing of gait in advanced PD patients, can bind α-syn and controls α-syn-mediated DA overflow and presynaptic compartmentalization. Interestingly, MPH results also efficient for the treatment of attention deficits and hyperactivity disorder (ADHD), a neurodevelopmental psychiatric syndrome associated with Syn III and α-syn polymorphisms and constituting a risk factor for the development of LB disorders.

Here, we studied α-syn/Syn III co-deposition and longitudinal changes of α-syn, Syn III and DA transporter (DAT) striatal levels in nigrostriatal neurons of a PD model, the human C-terminally truncated (1 − 120) α-syn transgenic (SYN120 tg) mouse, in comparison with C57BL/6J wild type (wt) and C57BL/6JOlaHsd α-syn null littermates. Then, we analyzed the locomotor response of these animals to an acute administration of MPH (d-*threo*) and other MRIs: cocaine, that we previously found to stimulate Syn III-reliant DA release in the absence of α-syn, or the selective DAT blocker GBR-12935, along aging. Finally, we assessed whether these drugs modulate α-syn/Syn III interaction by fluorescence resonance energy transfer (FRET) and performed *in silico* studies engendering a heuristic model of the α-syn conformations stabilized upon MPH binding.

We found that only MPH was able to over-stimulate a Syn III-dependent/DAT-independent locomotor activity in the aged SYN120 tg mice showing α-syn/Syn III co-aggregates. MPH enhanced full length (fl) α-syn/Syn III and even more (1–120) α-syn/Syn III interaction in cells exhibiting α-syn/Syn III inclusions. Moreover, *in silico* studies confirmed that MPH may reduce α-syn fibrillation by stabilizing a protein conformation with increased lipid binding predisposition.

Our observations indicate that the motor-stimulating effect of MPH can be positively fostered in the presence of α-syn/Syn III co-aggregation. This evidence holds significant implications for PD and ADHD therapeutic management.

* Corresponding author at: Division of Pharmacology, Department of Molecular and Translational Medicine, University of Brescia, Viale Europa 11, 25123 Brescia, Italy.

E-mail addresses: g.faustini004@unibs.it (G. Faustini), f.longhena@unibs.it (F. Longhena), federica.bono@unibs.it (F. Bono), luca.lavia@unibs.it (L. La Via), alessandro.barbon@unibs.it (A. Barbon), andrea.casiraghi@unimi.it (A. Casiraghi), valentina.straniero@unimi.it (V. Straniero), ermanno.valoti@unimi.it (E. Valoti), gabriele.costantino@unipr.it (G. Costantino), fabio.benfenati@iit.it (F. Benfenati), mariacristina.missale@unibs.it (C. Missale), marina.pizzi@unibs.it (M. Pizzi), mgs11@cam.ac.uk (M.G. Spillantini), arianna.bellucci@unibs.it (A. Bellucci).

https://doi.org/10.1016/j.nbd.2020.104789
Received 7 November 2019; Received in revised form 20 January 2020; Accepted 31 January 2020
Available online 04 February 2020

1. Introduction

Synapsin III (Syn III) is a synaptic phosphoprotein negatively regulating striatal dopamine (DA) release by cooperating with α-synuclein (α-syn) (Hosaka and Sudhof, 1998; Kile et al., 2010; Zaltieri et al., 2015). We recently described that in Parkinson's disease (PD), the most common neurodegenerative movement disorder, characterized by progressive loss of dopaminergic neurons of the *substantia nigra*, Syn III associates with α-syn to compose the insoluble fibrils forming Lewy Bodies (LB) (Longhena et al., 2018; Spillantini et al., 1997). Aggregation and deposition of α-syn at synaptic sites are considered as the *primum movens* for the derangement of dopaminergic neurons in PD (Bellucci et al., 2016). Our recent findings support that, besides composing α-syn insoluble fibrils, Syn III acts as a crucial mediator of α-syn aggregation and toxicity. Indeed, Syn III knock out (ko) mice do not develop α-syn insoluble aggregates and the related degeneration of dopaminergic nigrostriatal neurons prompted by the adeno-associated virus (AAV)-induced overexpression of human wild type (wt) α-syn (Faustini et al., 2018).

Syn III regulates DA release and is the only synapsin co-localizing with vesicular monoamine transporter 2 (VMAT2) in the *striatum* (Bogen et al., 2006; Faustini et al., 2018). Our previous studies indicating that Syn III is up-regulated in the absence of α-syn in mesencephalic dopaminergic neurons subjected to α-syn gene silencing, or produced from α-syn null mice (C57BL/6JOlaHsd), support the existence of a crucial interplay between Syn III and α-syn (Zaltieri et al., 2015). The compensatory increase of Syn III observed in mice lacking α-syn mediates a paradoxical over-response to the administration of the monoamine reuptake inhibitor (MRI) cocaine, which can stimulate synapsin-dependent DA release (Venton et al., 2006). Contrariwise, the selective DA transporter (DAT) blocker GBR-12935 does not exert the same effect (Zaltieri et al., 2015).

Twelve-month-old transgenic mice, overexpressing C-terminally truncated (1–120) α-syn (SYN120 tg) under the guidance of rat tyrosine hydroxylase (TH) promoter, on the mouse C57BL/6JOlaHsd α-syn null background, show a marked co-accumulation of α-syn and Syn III in the *striatum* (Zaltieri et al., 2015), similarly to PD patients (Longhena et al., 2018). These mice progressively develop α-syn insoluble aggregates in dopaminergic nigrostriatal neurons from 2 months of age. At 12 months of age, they exhibit reduced basal and K^+-stimulated striatal DA release associated with redistribution of soluble NSF attachment protein receptor (SNARE) proteins and DAT, without a frank dopaminergic cell loss (Bellucci et al., 2011; Garcia-Reitbock et al., 2010; Tofaris et al., 2006). Amphetamine-induced motor abnormalities are also detected at 18 months of age (Tofaris et al., 2006). Thus, this transgenic mouse line constitutes a progressive model of PD, recapitulating the earliest α-syn-related synaptic derangement of dopaminergic neurons that may initiate neuronal loss (Garcia-Reitbock et al., 2010). This is in line with evidence supporting the relevance of truncated α-syn in the early pathogenic steps leading to LB formation (Prasad et al., 2012). Indeed, the core of LB is enriched in C-terminally truncated α-syn (Prasad et al., 2012), which assembles into filaments and forms inclusions much more readily than full length (fl), wt or mutated protein (Crowther et al., 1998; Fares et al., 2016).

Methylphenidate (MPH), a MRI currently used for the treatment of attention deficits and hyperactivity disorder (ADHD) (Huss et al., 2017), that can be associated with Syn III or α-syn polymorphisms (Basay et al., 2016; Gerlach et al., 2019; Kenar et al., 2013), has been found to efficiently counteract freezing of gait in advanced PD (Delval et al., 2015; Devos et al., 2007; Moreau et al., 2012; Nikolai Gil D. Reyes, 2018; Pollak et al., 2007). Notably, MPH displays α-syn binding ability and results able to stimulate α-syn-mediated DA neurotransmission (Chadchankar et al., 2012; Kile et al., 2010; Venton et al., 2006), supporting that α-syn/Syn III interplay may influence the effect of this drug. The aim of this study was to assess whether and how the formation of α-syn/Syn III co-aggregates in SYN120 tg mice may affect the locomotor response to MPH.

To this purpose, we first characterized Syn III accumulation within thioflavin S/α-syn-positive inclusions in the nigrostriatal neurons of SYN120 tg mice. Then, we evaluated how α-syn expression and aggregation may affect Syn III and DAT levels in the *striatum* and studied in parallel MPH-, cocaine- and GBR-12935-stimulated locomotor activity in C57BL/6J, C57BL/6JOlaHsd and SYN120 tg mice along aging. Finally, we investigated whether these drugs can affect α-syn/Syn III interaction in cells displaying α-syn/Syn III co-aggregates and performed *in silico* studies to confirm stable binding between MPH and either human fl or C-terminally truncated α-syn. Our results support that the pathological α-syn/Syn III co-deposition produces a synaptic microenvironment engendering the formation of specific α-syn conformational variants boosting a Syn III-dependent motor response to MPH.

2. Material and methods

2.1. Animals

C57BL/6J wt mice (Charles River, Wilmington, MA), C57BL/6JOlaHsd carrying a spontaneous deletion of α-syn gene (Harlan Olac, Bicester, UK) and SYN120 tg mice (Tofaris et al., 2006) were used in this study at 3, 8, 12, 16 months of age. Syn III ko mice were analyzed at 12 months of age. Mice were bred in our animal house facility at the Department of Molecular and Translational Medicine of University of Brescia. Animals were maintained under a 12 h light–dark cycle at a room temperature (rt) of 22 °C and had ad libitum food and water. All experiments were made in accordance to Directive 2010/63/EU of the European Parliament and of the Council of 22 September 2010 on the protection of animals used. All experimental and surgical procedures conformed to the National Research Guide for the Care and Use of Laboratory Animals were approved by the Animal Research Committees of the University of Brescia (Protocol Permit 719/2015-PR). All achievements were made to minimize animal suffering and to reduce the number of animals used.

2.2. Animal surgery

The plasmids for the production of short hairpin (sh) AAV serotype 2/6 driven by the U6 promoter to silence the Syn III were acquired by Vector biolabs (Malvern, PA, USA).

Twelve-month-old SYN120 tg mice were bilaterally injected in the *substantia nigra* with either an AAV transducing an shRNA for Syn III gene silencing (AAV-shSyn III) or a scramble shRNA (AAV-shScramble) at a concentration of 10^{12} genome copies/ml. Briefly, animals were anesthetized and placed in a stereotactic head frame (Stoelting, IL, USA). After making a midline incision of the scalp, a hole was drilled in the appropriate location for the *substantia nigra* at the left and right site of the skull. Two microliters of AAV-shSyn III or AAV-shScramble were injected at a rate of 0.2 μl/min with a 33-gauge needle on a 10 μl Hamilton syringe at the following coordinates: antero-posterior – 3.70; medio-lateral + and – 1.50; dorsal-ventral – 3.9 relative to Bregma (Paxinos, 2012). The needle was left in place for additional 5 min before being slowly retracted from the brain. The locomotor activity of the AAV-shSynIII- and AAV-shScramble-inoculated mice was evaluated 4 months after the AAV injections.

2.3. Triple immunofluorescence staining

Twelve months old C57BL/6J, C57BL/6JOlaHsd and SYN120 tg mice were anesthetized with chloral hydrate 400 mg/kg intraperitoneal (i.p.) (Sigma-Aldrich, St. Louis, MO, USA) and transcardially perfused with ice-cold Immunofix (4% PFA, Bio-optica, Milan, Italy). Brains were post-fixed for 4 h in Immunofix and conserved in 18% sucrose (Sigma-Aldrich) in PBS 0.1 M. The brains were then cut in 25 μm coronal sections with a cryostat and conserved in 60% glycerol.

After permeabilization in PBS 0.1 M supplemented with 20% methanol and 0.3% Triton X-100, free floating slices were incubated for

5 h at rt. in strong blocking solution (10% Normal Goat Serum (NGS), 3% Bovine Serum Albumin (BSA), 0.05% NaN_3, 0.3% Triton-X100 in PBS 0.1 M) and then with the primary antibody in blocking solution overnight at 4 °C. The following day, slices were washed with 0.3% Triton-X100 PBS 0.1 M and incubated with the fluorochrome-conjugated secondary antibody in 0.3% Triton-X100 PBS 0.1 M plus 1 mg/ml BSA for 1 h at rt. After three washes in 0.3% Triton X-100 PBS, slices were incubated for 2 h at rt with the second primary antibody prepared in blocking solution, followed by incubation for 1 h at rt with the optimal fluorochrome-conjugated secondary antibody. The sections undergoing triple immunolabeling were further subjected to incubation with a third primary antibody for 2 h at rt followed by incubation for 1 h with the fluorochrome-conjugated secondary antibody. Finally, cell nuclei were counterstained with TO-PRO®-3 Iodide (To Pro, Thermo Fisher Scientific, Waltham, USA), a carbocyanine monomer nucleic acid stain with far-red fluorescence, and the slices were mounted onto superfrost slides using Vectashield mounting medium for fluorescence (Vector Laboratories, Burlingame, CA).

2.4. Thioflavin S staining

For thioflavin S staining, mouse brain sections were incubated with 0.05% of Thioflavin S (Sigma-Aldrich) in ethanol 50%, washed three times for 10 s in 80% ethanol as previously described (Faustini et al., 2018) and then blocked for subsequent immunostaining with the antibody against Syn III. Cell nuclei were counterstained with Hoechst 33258 dye, mounted and analyzed by using a confocal microscope.

2.5. In situ Proximity Ligation Assay (PLA) studies

The *in situ* PLA studies on mice tissues were performed by using the Duolink assay kit (O-LINK Bioscience, Upsalla, Sweden) with a protocol adapted from the manufacturer's instruction, as previously described (Faustini et al., 2018). Briefly, tissues were incubated with blocking solution for 1 h and then with the primary antibodies recognizing Syn III and α-syn at 1:500 dilution overnight at 4 °C. On the following day, samples were incubated with PLA probe solution for 1 h at 37 °C and with the ligation solution for 30 min at 37 °C, then with the amplification solution at 37 °C for 100 min. Finally, tissues were washed and subjected to another staining with TH antibody for 2 h at rt and probed with the secondary antibody. Cell nuclei were then counterstained with Hoechst 33258 dye and sections were mounted on slides and analyzed by using a confocal microscope.

2.6. Confocal microscopy

Slides were observed by LSM 880 Zeiss confocal laser microscope (Carl Zeiss S.p.A., Milan, Italy) with the following laser sets: λ = 405/488/543/633 nm for quadruple TH/α-syn/Syn III/To Pro staining, 488/543/405 for triple TH/PLA/Hoechst or 543/430/405 for Syn III/Thioflavin S/Hoechst staining. The height of sections scanning was 1 μm. Images (512 × 512 pixels) were then reconstructed using ZEISS ZEN Imaging Software (Carl Zeiss S.p.A.).

2.7. Image analysis of Syn III-immunopositive area in the substantia nigra

For the quantification of Syn III immunoreactivity in the *substantia nigra* the acquisition parameters during confocal imaging were maintained constant for all the images acquired to perform the analysis. Brains from 3 to 4 mice (10 sections from each mouse, two every 150 μm) were analyzed by examining the whole area of the *substantia nigra* within a virtual standard grid composed of 8 fields. The total Syn III-positive area within the grid was estimated by using the FIJI software. The mean of Syn III-positive area per section was calculated by averaging the values of the 10 grids analyzed for each animal in the different experimental groups. Values were then expressed as % changes vs C57BL/6J mice.

2.8. Western blot (WB) analysis

Fresh frozen tissues from the *striatum* were collected from mouse brains after cervical dislocation. Total proteins were extracted with Radioimmunoprepitation Assay (RIPA) buffer made up by 50 mM Tris-HCl pH 7.4, 150 mM NaCl, NP-40 1%, sodium deoxycholate 0.1%, sodium dodecyl sulfate (SDS) 0.1%, 1 mM NaF, 1 mM $NaVO_4$ plus complete protease inhibitor mixture (Roche Diagnostics, Mannheim, Germany). Protein concentration in the samples was measured by using the Bio-Rad DCTM protein assay kit (Bio-Rad Laboratories, Milan, Italy). Equal amounts of proteins (30 μg) were run on 10% polyacrylamide gels and transferred onto polyvinylidene fluoride (PVDF) membrane. Densitometric analysis of the bands were performed by using FIJI Software and all bands were normalized to Glyceraldehyde 3-phosphate dehydrogenase (GAPDH) levels as a control of equal loading of samples in the total protein extracts. For densitometry analysis of bands, each experimental condition was performed in quadruplicate and the resulting data were subjected to statistical analysis.

2.9. Real-time PCR

Total RNA was extracted from *substantia nigra* specimens of C57BL/6J, C57BL/6JOlaHsd and SYN120 tg mice using an RNA extraction kit (RNeasy Mini Kit, Qiagen, Hilden, GE) as previously described (Faustini et al., 2018). Two μg of RNA were retrotranscribed by using QuantiTect Reverse Transcription Kit (Qiagen) according to the manufacturer's instructions. Real-time PCR was performed by using SYBR Green Master Mix (Applied Biosystems, Foster City, USA) and the following primer pairs: *SYN3* for aaatcagcatcaccccaccc, *SYN3* rev gccttggcctcatcttcact; *GAPDH* for tcaacagcaactcccactctt, *GAPDH* rev ccagggtttcttactccttgg.

The ViiA7 Real Time PCR system (Life Technologies, Grand Island, NY, U.S.A.) as used for 40 cycles of 95 °C for 15 s and 60 °C for 1 min. mRNA expression was normalized to GAPDH gene expression. Each experimental condition was analyzed in triplicate and the resulting data were averaged and subjected to statistical analysis.

2.10. Antibodies

A list of the primary antibodies for detection of α-syn, DAT, GAPDH, Syn III and TH and of their working concentrations in immunofluorescence,

Table 1
List of the primary antibodies used for the study including their characteristics and working dilutions.

Antibody	Catalog number	Manufacturer	Clonality	Immunogen	Host species	Working dilution		
						WB	IF	*In situ* PLA
Alpha-syn (syn1)	610,787	BD	Monoclonal	aa. 15–123	Mouse	1:1000		1:500
DAT	AB2231	Millipore	Polyclonal	N-terminus	Rabbit	1:3000		
GAPDH	G8795	Sigma-Aldrich	Monoclonal	Not specified	Mouse	1:5000		
Syn III	106,303	Synaptic System	Polyclonal	aa 417–434	Rabbit	1:2000	1:600	1:500
TH	AB152	Millipore	Polyclonal	Not specified	Rabbit		1:700	

in situ PLA and WB studies is summarized in Table 1. The secondary antibodies used for fluorescence immunohistochemistry were a goat anti-mouse IgG Cy3-conjugated, a goat anti-rabbit IgG Cy3-conjugated, a goat anti-rabbit Alexa488-conjugated and a goat anti-rabbit Alexa405-conjugated (Jackson ImmunoResearch, Pennsylvania, USA). The secondary antibodies used for WB were goat anti-rabbit IgG-HRP or goat anti-mouse IgG-HRP (Santa Cruz Biotechnology, Dallas, Texas, USA).

2.11. Open field behavioral tests

Acute locomotor activity of C57BL/6J, C57BL/6JOlaHsd, SYN120 tg and Syn III ko mice was assessed using the automated AnyMaze video tracking system (Stoelting, Wood Dale, IL) according to previously described protocols (Zaltieri et al., 2015). The total distance travelled was recorded automatically in the open field arena (50 × 50 cm^2) and data were analyzed in 14 trials of 2.5 min each. Mice were gently placed in the arena and were allowed to explore freely for 5 min before starting the test. After 10 min of registration in basal condition, mice received an i.p. injection of cocaine (10 mg/kg, dissolved in normal saline 0.9%) (Tocris, Bristol, UK), or MPH (d-*threo*, 10 mg/kg, dissolved in normal saline 0.9%) (Tocris), or GBR-12935 (20 mg/kg, dissolved in normal saline 0.9%) (Tocris), whereas control mice were treated with vehicle (normal saline 0.9%). To evaluate the effect of MPH or cocaine independently of their DAT-inhibitory action, the protocol was adapted as follows. Mice were analyzed for 10 min in basal conditions, then subjected to an i.p. injection of GBR-12935 (20 mg/kg), registered for 15 min and finally subjected to an i.p. injection of either cocaine (10 mg/kg) or MPH (10 mg/kg) registering for the following 25 min. All the experiments were conducted during daylight hours. $N = 6/10$ animals per group were analyzed for each experimental setting including vehicle or drug treatments.

2.12. Acceptor photobleaching fluorescence resonance energy transfer (FRET) studies

Human neuroblastoma SK-N-SH cells were grown in complete medium comprising Dulbecco's modified Eagle's medium with 1000 mg glucose/l (Life technologies, California, USA) supplemented with 10% heat-inactivated fetal bovine serum, 100 μg/ml penicillin, 100 μg/ml streptomycin and 0.01 μM non-essential amino acids (Sigma-Aldrich). Cells were maintained at 37 °C under a humidified atmosphere of 5% CO_2 and 95% O_2.

For FRET studies, SK-N-SH cells were seeded onto poli-D-lysine-coated 13 mm glass coverslips in 24-well plates (15,000 cells per coverslip) and were maintained in differentiation medium for ten days by daily adding 10 μM retinoic acid to the complete medium. At day 7, cells were transiently transfected with pGFP-human Syn III (transducing human green fluorescent protein (GFP)-tagged Syn III and pCMV6-RFP-α-syn 140 (transducing red fluorescent protein (RFP)-tagged fl α-syn) or pCMV6-RFP-α-syn 120 (transducing RFP-tagged (1–120) α-syn) constructs, by using Lipofectamine 3000 (Life Technologies), according to the manufacturer's instructions. pCMV6-RFP-α-syn 140 or pCMV6-RFP-α-syn 120 single-transfected cells were used as negative controls during the FRET experiments. Three days after transfection, cells were treated for 15 min with vehicle (normal saline 0.9%), 10 μM cocaine, 10 μM MPH (d-threo) or 10 μM GBR-12935, then immediately fixed with Immunofix for 15 min and subsequently mounted on glass slides.

Fixed cells were analyzed by means of a Zeiss confocal laser microscope LSM 880 (Carl Zeiss) with the laser set on λ = 488–543.

After identifying double positive cells three-to-six regions of interest (ROI) were analyzed for 4 series. Two images of basal condition (Pre-bleaching) were acquired before bleaching the RFP acceptor fluorophore with laser 543 set at 65% power. Then, other two images were acquired after the bleaching (Post-bleaching).

The FRET efficiency (intended as the GFP recovery after RFP photobleaching) was measured by using Zen black software (Carl Zeiss). The average intensity of the background (outside the cell) was subtracted from the average intensity of the ROI and all the FRET values resulting from the different ROI were used for statistical analysis.

2.13. Molecular modeling of MPH interaction with either fl or C-terminally truncated α-syn

The frame number 4 of the nuclear magnetic resonance (NMR) structure of α-syn (2KKW) was used to pursue docking studies by means of Glide (https://www.schrodinger.com). The protein was prepared with the protein preparation tool of Maestro (https://www.schrodinger.com) and the docking grid was centered so as to cover the whole region where the N-terminal and C-terminal domains are in close proximity. MPH was prepared with the atom builder tool of Maestro. Each docking run was carried out using the standard precision (SP) method and the Van der Waals scaling factor of nonpolar atoms was set to 0.8. The binding mode having the highest score was selected after visual inspection. The (1–120) α-syn MPH complex was prepared starting from the generated model of fl α-syn in complex with MPH. The fl α-syn was then truncated at the 120^{th} residue and the complex thus obtained was submitted to a stepwise refinement protocol, where the complex was refined by applying harmonic constraints that were progressively reduced until no constraints were applied.

2.14. Statistical analysis

Statistical differences in the protein levels detected by WB or estimated by immunofluorescence and in mRNA expression between groups (C57BL/6J, C57BL/6JOlaHsd and SYN120 tg mice) were assessed by using one-way ANOVA followed by Bonferroni's multiple comparisons test ($n = 6$ animals for each group for WB and immunofluorescence analysis and $n = 3$ animals for each group for qPCR analysis). Statistical differences between the total distance travelled in the open field test by the different experimental groups (C57BL/6J, C57BL/6JOlaHsd and SYN120 tg or Syn III ko and wt mice or SYN120 tg mice injected with AAV-shSyn III and AAV-shScramble) were assessed by using two-way ANOVA followed by Bonferroni's multiple comparisons test ($n = 6$–12 animals for each group). Differences in the mean FRET efficiencies of SK-N-SH cells were assessed by using one-way ANOVA + Newman-Keuls post comparison test ($n = 15$–20 cells for each experimental condition). Differences in the Syn III immunopositive area in the *substantia nigra* between SYN120 tg mice injected with scramble shRNA or shRNA for Syn III gene silencing were analyzed by Student's *t*-test. All data are presented as mean ± standard error of the mean (SEM) and statistical significance was established at $P < 0.05$.

3. Results

3.1. Synapsin III deposition and interaction with α-syn in the substantia nigra

We recently showed that 12-month-old C57BL/6JOlaHsd α-syn null mice display striatal redistribution and accumulation of Syn III when compared to C57BL/6J littermate controls (Zaltieri et al., 2015). The Syn III alterations are even more pronounced in the *striatum* of 12-month-old SYN120 tg mice overexpressing C-terminally truncated α-syn on the C57BL/6JOlaHsd background (Zaltieri et al., 2015), which at this age exhibit a marked deposition of fibrillary aggregated α-syn as well as SNAREs and DAT redistribution accompanied by DA release failure, as we previously showed (Bellucci et al., 2011; Garcia-Reitbock et al., 2010; Tofaris et al., 2006). Here, we investigated Syn III immunolabeling and co-localization with Thioflavin S-positive fibrillary aggregates in the *substantia nigra* TH-positive neurons of 12-month-old SYN120 tg vs. C57BL/6J or C57BL/6JOlaHsd mice in order to evaluate the presence of Syn III within α-syn aggregates in this brain area. In line with our previous findings on striatal sections (Zaltieri et al., 2015),

confocal analysis showed accumulation of Syn III in *substantia nigra* TH-positive neurons of C57BL/6JOlaHsd α-syn null and even more in those of SYN120 tg mice, with respect of C57BL/6J littermates (Fig. 1A-C; Supplementary Fig. 1A). While in the nigral TH-positive cells of α-syn null mice Syn III immunoreactivity displayed a dot-like sparse distribution (Fig. 1B, arrows), in those of SYN120 tg mice it exhibited a more condensed dot-like or mealy-granular appearance (Fig. 1C arrows) and showed a marked co-localization with α-syn (Fig. 1C merge). In C57BL/6J mice, Syn III staining was poor (Fig. 1A).

We then assessed α-syn and Syn III interaction in the *substantia nigra* TH-positive neurons by *in situ* PLA (Fig. 1D-F), which allows to visualize protein-protein interactions in intact tissues (Bellucci et al., 2014; Faustini et al., 2018). We found that 12-month-old C57BL/6J mice exhibited a basal α-syn/Syn III PLA signal supportive of the occurrence of Syn III/α-syn interaction (Fig. 1D). The PLA signal was increased in the nigral TH-positive cells of SYN120 tg mice (Fig. 1F), suggesting an augmented interaction between C-terminally truncated (1–120) α-syn and Syn III. The absence of PLA staining in the *substantia nigra* of C57BL/6JOlaHsd mice (Fig. 1E) confirmed the specificity of the assay.

As stated above, 12-month-old SYN120 tg mice exhibit α-syn fibrillary aggregation in the *substantia nigra* (Tofaris et al., 2006). Here, we observed a marked co-localization between Syn III immunolabeling and Thioflavin S staining in both the *substatina nigra* and *striatum* that supports the presence of Syn III within the fibrillary α-syn aggregates in the nigrostriatal neurons of these mice (Fig. 2).

3.2. Age-related changes in Syn III and DAT levels in the striatum of C57BL/6J, C57BL/6JOlaHsd and SYN120 tg mice

The age-dependent changes in α-syn, DAT and Syn III levels in the *striatum* of C57BL/6J, C57BL/6JOlaHsd and SYN120 tg mice were assessed at 3, 8, 12 and 16 months of age (Fig. 3) by WB.

In line with our previous findings (Tofaris et al., 2006), we observed that the expression of C-terminally truncated α-syn in SYN120 tg mice was lower than fl wt α-syn in the C57BL/6J littermate controls (Fig. 3). Indeed, the expression of (1–120) α-syn in SYN120 tg mice is under the control of the rat TH promoter and is thus restricted to striatal dopaminergic terminals. The C57BL/6JOlaHsd mice did not show α-syn (Fig. 3).

At 3 months of age, DAT levels were decreased in C57BL/6JOlaHsd mice when compared to both C57BL/6J and SYN120 tg littermates. However, this difference was abated in 8-month-old animals (Fig. 3). We then found that in SYN120 tg mice, DAT levels were significantly augmented at 12 and 16 months of age, when compared to control C57BL/6JOlaHsd littermates. This augment in DAT levels cannot be indicative of increased dopaminergic projections in the *striatum*, as supported by the significant decrease of basal and depolarization-dependent DA release and of its main metabolites 3, 4-dihydroxyphenylacetic acid (DOPAC) and homovanillic acid (HVA) that we previously described in the SYN120 tg mice from 12 months of age (Garcia-Reitbock et al., 2010). It can rather be ascribed to other compensatory mechanisms regulating the DAT in response to DA release

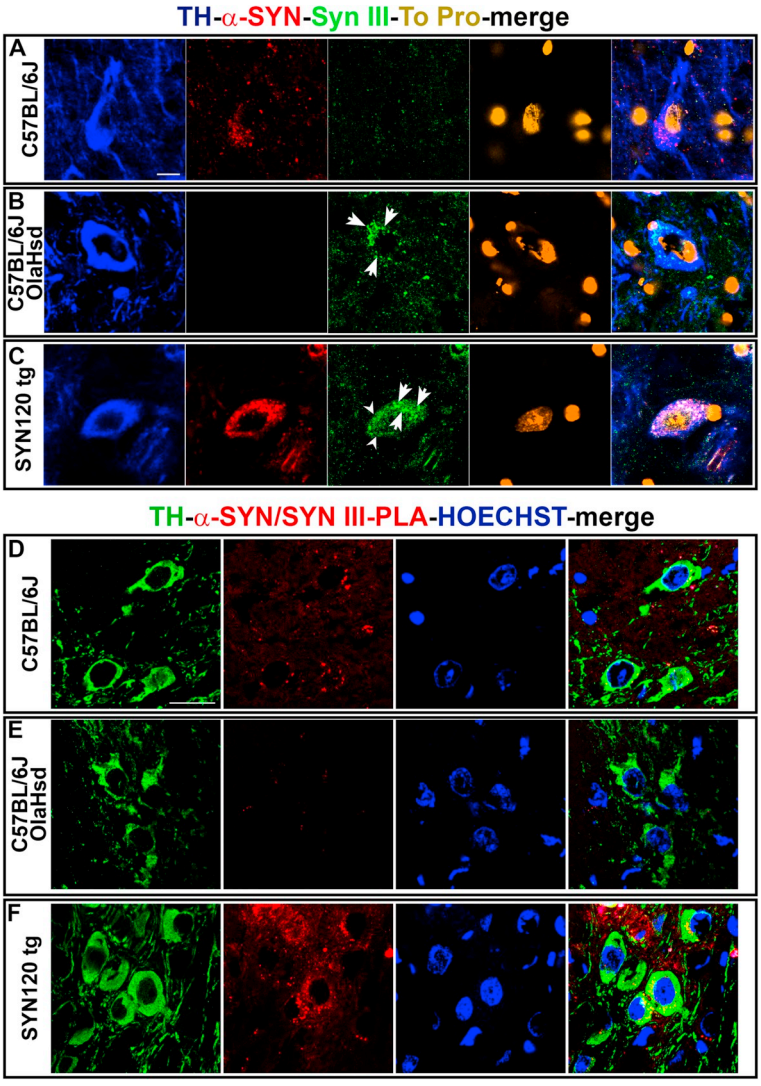

Fig. 1. Immunofluorescence labeling of α-syn and Syn III and *in situ* PLA in TH-positive *substantia nigra* neurons of 12-month-old C57BL/6J, C57BL/6JOlaHsd and SYN120 tg mice.
A. Mild α-syn and Syn III staining in the TH-positive cells of C57BL/6J mice. B. Marked accumulation of Syn III (white arrows) within the TH-positive cells of C57BL/6JOlaHsd mice which did not exhibit α-syn immunoreactivity. C. Marked accumulation of α-syn and Syn III (white arrows) in the TH-positive neurons of SYN120 tg mice. Cell nuclei were counterstained with To Pro. Scale bar 10 μm.
D. Presence of a mild α-syn/Syn III in situ PLA positivity in the TH-positive neurons of C57BL/6J mice. E. Absence of the α-syn/Syn III *in situ* PLA signal in the TH-positive cells of C57BL/6JOlaHsd mice. F. The accumulation of the α-syn/Syn III *in situ* PLA reactivity in the TH-positive neurons of SYN120 tg mice is supportive of the improvement of α-syn/Syn III interaction. Cell nuclei were counterstained with HOECHST. Scale bar 10 μm.

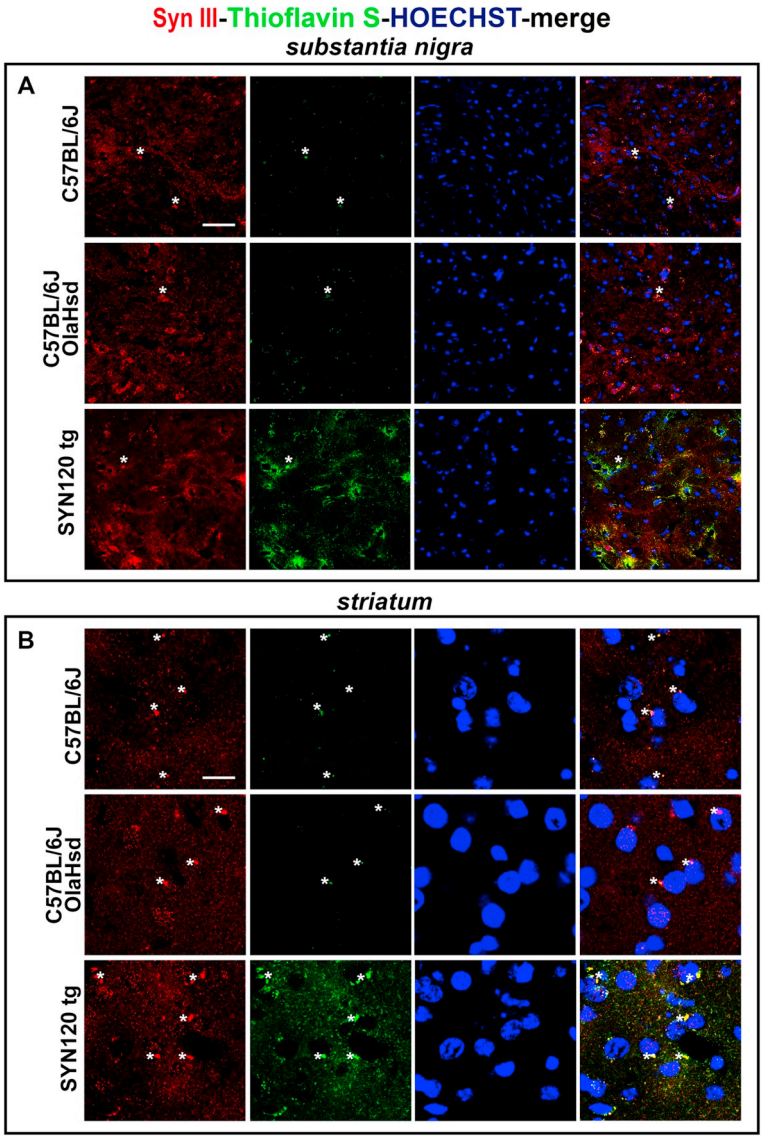

Fig. 2. Syn III immunolabeling coupled with Thioflavin S staining in the *substantia nigra* and *striatum* of 12-month-old C57BL/6J, C57BL/6JOlaHsd and SYN120 tg mice.

A. Marked accumulation of the Thioflavin S signal, indicative of protein fibrillation, in co-localization with Syn III immunopositive labeling in the *substantia nigra* of SYN120 tg mice. B. Marked Syn III and Thioflavin S co-localizing signals were also observed in the *striatum* of SYN120 tg mice. Please note that asterisks are located nearby non-specific lipofuscin signal. Scale bar A: 100 μm, B: 10 μm.

failure or α-syn aggregation. Consistently, in line with the results we report here and our previous findings (Bellucci et al., 2011), a recent study showed the occurrence of DAT upregulation and α-syn/DAT complexes formation as early pathological events in non-human primates who received putaminal injection of α-syn preformed fibrils and exhibiting loss of nigrostriatal neurons (Chu et al., 2019).

We then observed that, at 3, 8 and 12 months of age, the absence of α-syn induced a statistically significant increase of Syn III in C57BL/6JOlaHsd mice when compared to the C57BL/6J littermates. At 3 and 8 months of age, the levels of Syn III were reduced in SYN120 tg mice when compared to C57BL/6JOlaHsd littermates, suggesting that the presence of α-syn, even if in the truncated form, may attenuate the massive increase of Syn III. This notwithstanding, SYN120 tg mice exhibited a progressive increase of Syn III levels which was comparable to that of C57BL/6JOlaHsd animals at later time points (Fig. 3). Since aggregation of (1–120) α-syn has been detected from 6 months of age in the brains of SYN120 tg mice (Tofaris et al., 2006), it is feasible that the early down-regulation of Syn III levels in the *striatum* may be ascribed to the enhanced production of soluble C-terminally truncated α-syn which might later lose this action when fibrillation begins.

To further corroborate whether the expression of C-terminally truncated α-syn on the C57BL/6JOlaHsd background could quench Syn III expression similarly to wt protein in C57BL/6J mice, we assessed Syn III mRNA levels by real-time quantitative PCR at 3 and 12 months of age (Supplementary Fig. 1B). At 3 months of age, the expression of Syn III mRNA was significantly increased in C57BL/6JOlaHsd mice when compared to wt mice. In parallel, Syn III expression in the SYN120 tg mice was decreased vs C57BL/6JOlaHsd and increased vs C57BL/6J littermates, but these changes did not result statistically significant. At 12 months of age, the differences in relative Syn III mRNA expression observed between C57BL/6J, C57BL/6JOlaHsd and SYN120 tg mice mirrored the changes in protein levels detected by WB (Supplementary Fig. 1B).

Although the decrease of Syn III mRNA observed in SYN120 tg mice at 3 months of age did not exactly retrace the reduction of the protein, as detected by WB, it is known that mRNA amount will not always reflect the level of the encoded protein. Indeed, the amount of mRNA within a cell is determined by the ratio of its synthesis and degradation rates, which are finely regulated processes (Mattick, 2004). Moreover,

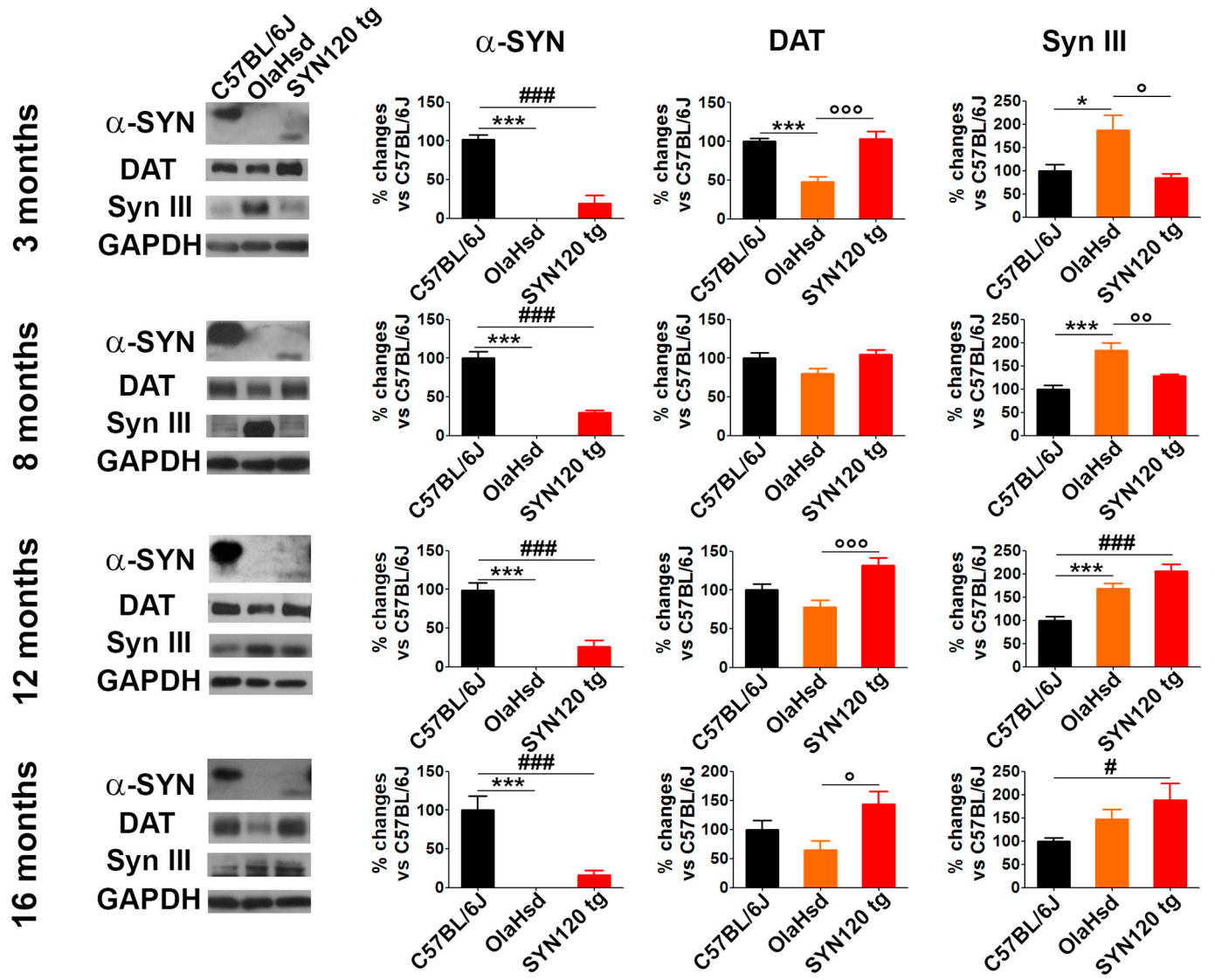

Fig. 3. Analysis of the levels of α-syn, DAT and Syn III in the *striatum* of C57BL/6J, C57BL/6JOlaHsd and SYN120 tg mice at 3, 8, 12, 16 months of age. The expression of (1–120) α-syn in SYN120 tg mice resulted lower than that of endogenous wt α-syn in C57BL/6J littermate controls at all the time point analyzed (### $P < 0.001$, One-way ANOVA + Bonferroni's post-comparison test). C57BL/6J exhibited a statistically significant difference in α-syn immunopositivity when compared to C57BL/6JOlaHsd littermates which did not exhibit α-syn immunopositivity (*** $P < 0.001$, One-way ANOVA + Bonferroni's post-comparison test). Three-month-old C57BL/6JOlaHsd mice displayed decreased DAT levels when compared to both C57BL/6J (*** - 52.66%, $P < 0.001$, One-way ANOVA + Bonferroni's post-comparison test) and SYN120 tg mice (°°° -55.78%, $P < 0.001$, One-way ANOVA + Bonferroni's post-comparison test). These differences were lost at 8 months of age. The levels of DAT resulted significantly increased in 12- and 16-month-old SYN120 tg mice when compared to C57BL/6JOlaHsd littermates (°°° + 53.73%, $P < 0.001$ and ° + 79.04%, $P < 0.05$, One-way ANOVA + Bonferroni's post-comparison test). A significant increase of Syn III levels was observed in C57BL/6JOlaHsd mice when compared to C57BL/6J littermates at 3, 8 and 12 months of age (* + 87.65%, $P < 0.05$ at 3 months and *** + 82.86% at 8 months, *** + 68.38% at 12 months, $P < 0.001$, One-way ANOVA + Bonferroni's post-comparison test). At 3 and 8 months of age, the levels of Syn III in SYN120 tg mice were comparable to those of C57BL/6J littermates, but resulted significantly reduced when compared to C57BL/6JOlaHsd mice (° - 103.5%, $P < 0.05$ at 3 months and °° - 54.54%, $P < 0.01$ at 8 months, One-way ANOVA + Bonferroni's post-comparison test). This notwithstanding, at 12 and 16 months SYN120 tg mice showed an age-related increase in Syn III levels, which returned comparable to those of C57BL/6JOlaHsd mice but were significantly augmented when compared to C57BL/6J littermates (### + 106.3%, $P < 0.001$ at 12 months and # + 88.57%, $P < 0.05$ at 16 months, One-way ANOVA + Bonferroni's post-comparison test).

WB analysis was conducted on striatal samples, while for qPCR experiments we used *substantia nigra* samples, as synapsins are synthesized in neuronal soma and then transferred to terminals through axonal transport (Tang et al., 2013).

3.3. Alpha-synuclein and Syn III interplay influences the locomotor response to MPH

We then wanted to expand our previous studies on the effect of cocaine administration in 12-month-old wt and C57BL/6JOlaHsd mice (Zaltieri et al., 2015) in order to evaluate the effect of different MRIs in these mouse lines and SYN120 tg animals at the time points used for the investigation of striatal proteins levels. In particular, we analyzed the acute locomotor response to the i.p. administration of cocaine (10 mg/kg), MPH (10 mg/kg, d-*threo*), GBR-12935 (20 mg/kg) or vehicle in C57BL/6J, C56BL/6JOlaHsd and SYN120 tg mice by using the open field behavioral paradigm (Zaltieri et al., 2015). We registered the distance travelled by mice in 2.5 min intervals for 10 min in basal condition and for 25 min after the i.p. administration of the drugs.

At 3 months of age, C57BL/6J mice exhibited a significant improvement of locomotion after cocaine administration, while C57BL/6JOlaHsd mice did not respond (Fig. 4A), in agreement with the fact

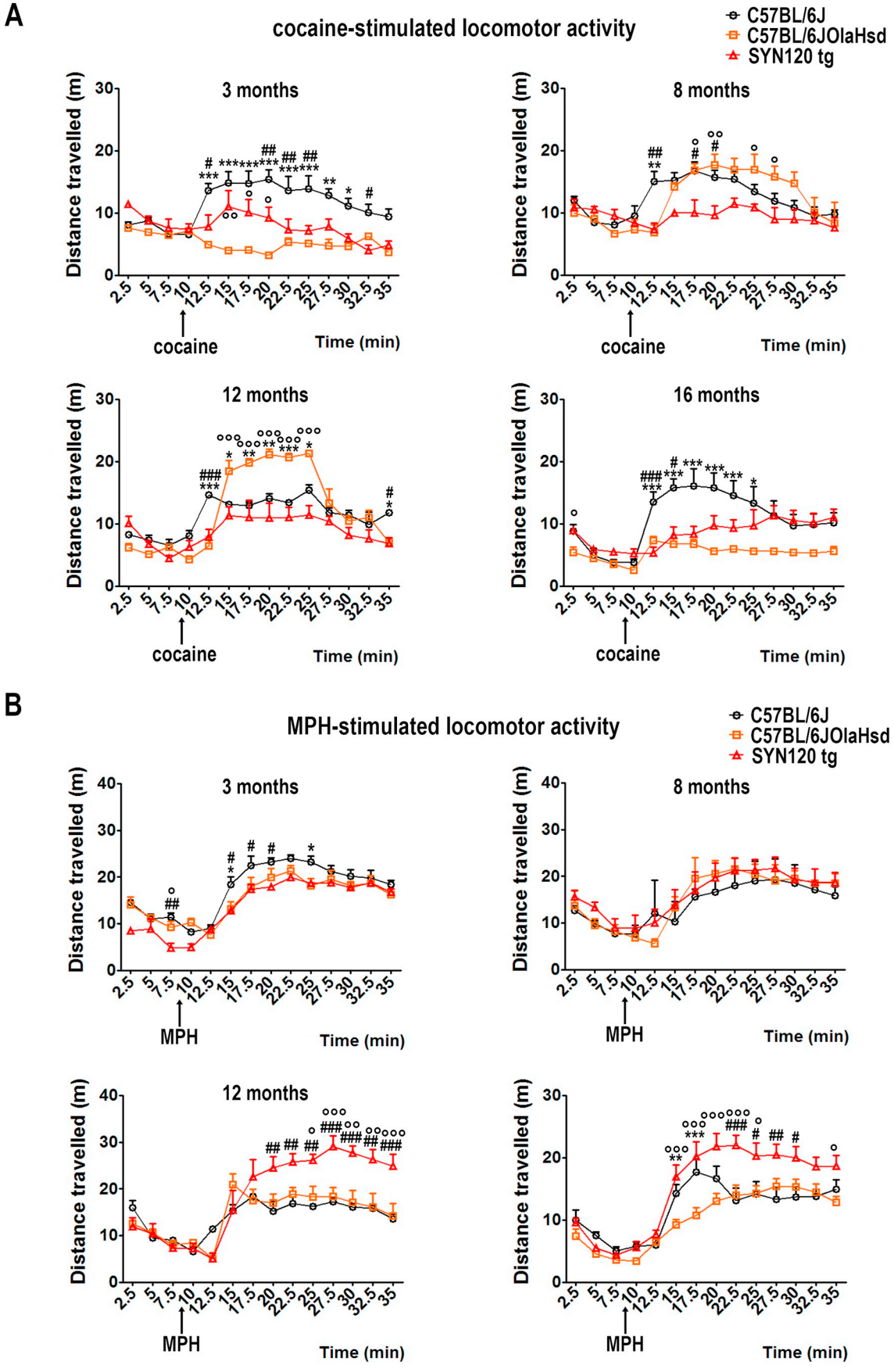

(caption on next page)

Fig. 4. Effect of cocaine or MPH administration on the locomotor activity of C57BL/6J, C57BL/6JOlaHsd and SYN120 tg mice at 3, 8, 12 and 16 months of age.
A. Cocaine differentially affected the locomotor response of C57BL/6J, C57BL/6JOlaHsd and SYN120 tg mice at all the time point analyzed (3 months: interaction: $F_{26,180} = 3.139$: 8 months: interaction: $F_{26,210} = 2.652$, $P < 0.0001$; 12 months: interaction: $F_{65,286} = 7.120$, $P < 0.0001$; 16 months: interaction: $F_{26,340} = 2.538$ $P < 0.001$). At 3 and 16 months of age C57BL/6J mice showed an enhanced locomotor response to cocaine vs C57BL/6JOlaHsd (*** $P < 0.001$, ** $P < 0.01$, * $P < 0.05$) or SYN120 tg littermates (# $P < 0.05$, ## $P < 0.01$, ### $P < 0.001$). At 3 months of age these latter showed a mild statistically significant increase in the locomotor response to cocaine vs C57BL/6JOlaHsd mice (° $P < 0.05$, °° $P < 0.01$). At 8 months of age, the locomotor response of C57BL/6JOlaHsd mice to cocaine administration was comparable to that observed in C57BL/6J animals, but out matched that of SYN120 tg mice (° $P < 0.05$, °° $P < 0.01$). Twelve-month-old C57BL/6JOlaHsd mice exhibited a significant increase in the locomotor response to cocaine vs wt littermates (*** $P < 0.001$, ** $P < 0.01$, * $P < 0.05$) and SYN120 tg mice (° $P < 0.05$, °° $P < 0.01$, °°° $P < 0.001$). Finally, at 16 months of age only C57BL/6J mice were able to display a locomotor response to cocaine administration and exhibited significant differences vs both C57BL/6JOlaHsd (*** $P < 0.001$, * $P < 0.05$) and SYN120 tg mice (### $P < 0.001$), which showed comparable feedbacks.
B. MPH differentially affected the locomotor response of C57BL/6J, C57BL/6JOlaHsd and SYN120 tg mice at all the time point analyzed (3 months: interaction: $F_{26,210} = 1.553$, $P < 0.05$; 8 months: interaction: $F_{26,82} = 0.2541$; 12 months: interaction: $F_{26,210} = 3.901$, $P < 0.0001$; 16 months: interaction: $F_{26,405} = 2.299$ $P < 0.001$). At 3 months of age C57BL/6J mice exhibited a mild increase in MPH-stimulated motility vs C57BL/6JOlaHsd (* $P < 0.05$) and SYN120 tg mice (# $P < 0.05$, ## $P < 0.01$), which behaved similarly. At 8 months of age, the three mouse lines showed similar responses. At 12 and 16 months of age SYN120 tg mice exhibited a statistically significant improvement in the locomotor response to MPH administration vs C57BL/6J (# $P < 0.05$, ## $P < 0.01$ and ### $P < 0.001$) and C57BL/6JOlaHsd littermates (°° $P < 0.01$ and °°° $P < 0.001$). Sixteen-month-old C57BL/6J mice showed a brief statistically significant increase in the locomotor response at 5 and 7.5 min from MPH injection when compared to C57BL/6JOlaHsd mice (** $P < 0.01$ and *** $P < 0.001$).

that they display both reduced DAT levels and a marked increase of Syn III. Interestingly, 3-month-old SYN120 tg mice showed a significantly higher locomotor activity 5, 7.5 and 10 min after cocaine administration when compared to C57BL/6JOlaHsd littermates. This suggests that, in spite of the C57BL/6JOlaHsd background, the expression of C-terminally truncated α-syn in TH-positive neurons of 3-month-old SYN120 tg mice sustained a mild response to cocaine.

In agreement with the WB data, supporting a rebalance of DAT levels in the three mouse lines at 8 months of age, we found that C57BL/6JOlaHsd mice exhibited a statistically significant increase in the distance travelled in the interval between 7.5 and 17.5 min after cocaine administration, when compared to SYN120 tg mice, which lost the mild locomotor response observed at 3 months of age. The increase in motility observed in 8-month-old C57BL/6JOlaHsd mice following cocaine administration, that was not detected in the animals at 3 months of age, may be ascribed to striatal DAT increase in conjunction with elevated Syn III levels, as these proteins can additively contribute to raise the response to this drug. Indeed, Kile and co-authors showed that only single Syn III ko mice exhibit enhanced striatal dopaminergic functions but in parallel that cocaine-stimulated DA release is reduced in synapsin I/II/III triple ko animals (Kile et al., 2010). This supports that, although Syn III is the only synapsin exerting a negative regulatory control of DA release in the *striatum*, cocaine effect is reduced in the absence of Syn III but can instead be enhanced by the increase of this protein. This outcome may have worked in concert with a more marked cocaine-induced DA re-uptake inhibition related to DAT increase to uplift the locomotor response of the α-syn null mice at 8 months of age.

In line with this hypothesis and our previous observations (Zaltieri et al., 2015), when we studied the locomotor response to cocaine administration at 12 months of age, we found that C57BL/6JOlaHsd mice exhibited a delayed increase in their peak of motility, which however was significantly higher vs that observed in C57BL/6J wt mice, and rapidly dropped in the interval between 15 and 17.5 min after cocaine administration. This supports that, with the prolonged absence of α-syn, the kinetic of Syn III-dependent DA release may differ from the standard DAT-mediated effect. Again, 12-month-old SYN120 tg mice did not respond to cocaine administration, supporting that the significant increase of striatal DAT levels is not sufficient to recover the response to cocaine. This may be explained by the fact that these mice show a marked reduction of striatal DA release as well as alterations in the distribution of Syn III, DAT and SNARE proteins (Bellucci et al., 2011; Garcia-Reitbock et al., 2010; Zaltieri et al., 2015).

At 16 months of age, C57BL/6JOlaHsd mice lost their ability to respond to the acute cocaine treatment, suggesting that they lost their dopaminergic striatal functions along aging. Indeed, nigrostriatal neurons from α-syn ko mice may exhibit a lower vulnerability threshold during aging. In particular, they show reduction of TH-positive fibers in the *striatum* and decrease of striatal levels of TH and DAT accompanied by decrease of DA and its metabolites, without any change in the overall number of TH-positive neurons in the *substantia nigra* (Al-Wandi et al., 2010; Connor-Robson et al., 2016). Finally, we found that the locomotor response of 16-month-old C57BL/6J and SYN120 tg mice was almost comparable to that observed at 12 months of age.

We then studied the motor response of mice to MPH administration (Fig. 4B). At 3 and 8 months of age, SYN120 tg, C57BL/6JOlaHsd and C57BL/6J mice similarly responded to MPH administration in spite of the differences in DAT and Syn III levels (Fig. 4B). Surprisingly, at 12 months of age, SYN120 tg mice manifested a paradoxical and statistically significant motility increase when compared to C57BL/6J and C57BL/6JOlaHsd littermates, which showed comparable behaviors. The hyper-response to MPH administration of SYN120 tg mice persisted at 16 months of age, when also C57BL/6J mice exhibited a mild peak in the locomotor response in the first ten minutes following MPH administration, while C57BL/6JOlaHsd mice showed the same kind of motility observed at younger ages. These findings support that the locomotor response to MPH administration is enhanced in the presence of C-terminally truncated α-syn aggregates, when these are occurring in parallel to the increase of Syn III and DAT, in spite of the co-aggregation of these proteins with α-syn.

In order to estimate the exact contribution of DAT inhibition to the locomotor response of mice along aging, we also evaluated their motility following GBR-12935 administration (Supplementary Fig. 2A). In line with the decreased DAT levels observed in C57BL/6JOlaHsd and with our previous observation (Bellucci et al., 2011), we found a decreased activity of C57BL/6JOlaHsd and SYN120 tg mice when compared to C57BL/6J control mice at all the time point analyzed. This suggests that the formation of α-syn/DAT inclusions induces an impairment of DAT trafficking in SYN120 tg mice. Indeed, in line with evidence supporting a direct interaction between the central region of α-syn (aa 61–95) and DAT C-terminus (Lee et al., 2001), we and others have shown that α-syn affects DAT surface expression (Adamczyk et al., 2006; Bellucci et al., 2008; Chu et al., 2019; Fountaine and Wade-Martins, 2007; Wersinger and Sidhu, 2003; Wersinger and Sidhu, 2005). Among the synucleins, α-syn results the most efficient in negatively regulating physiological DAT transport to the plasma membrane (Oaks et al., 2013). Therefore, although we observed increased levels of DAT in SYN120 tg mice vs α-syn null littermates, the lower response to GBR-12935 that they exhibited could result from an α-syn-induced decrease of DAT membrane transport efficiency occurring in response to (1–120) α-syn expression on the C57BL/6JOlaHsd α-syn null background, that may have been worsened by the progressive aggregate formation.

During all the behavioral tests, parallel groups of C57BL/6J, C57BL/6JOlaHsd and SYN120 tg mice were injected with vehicle (normal

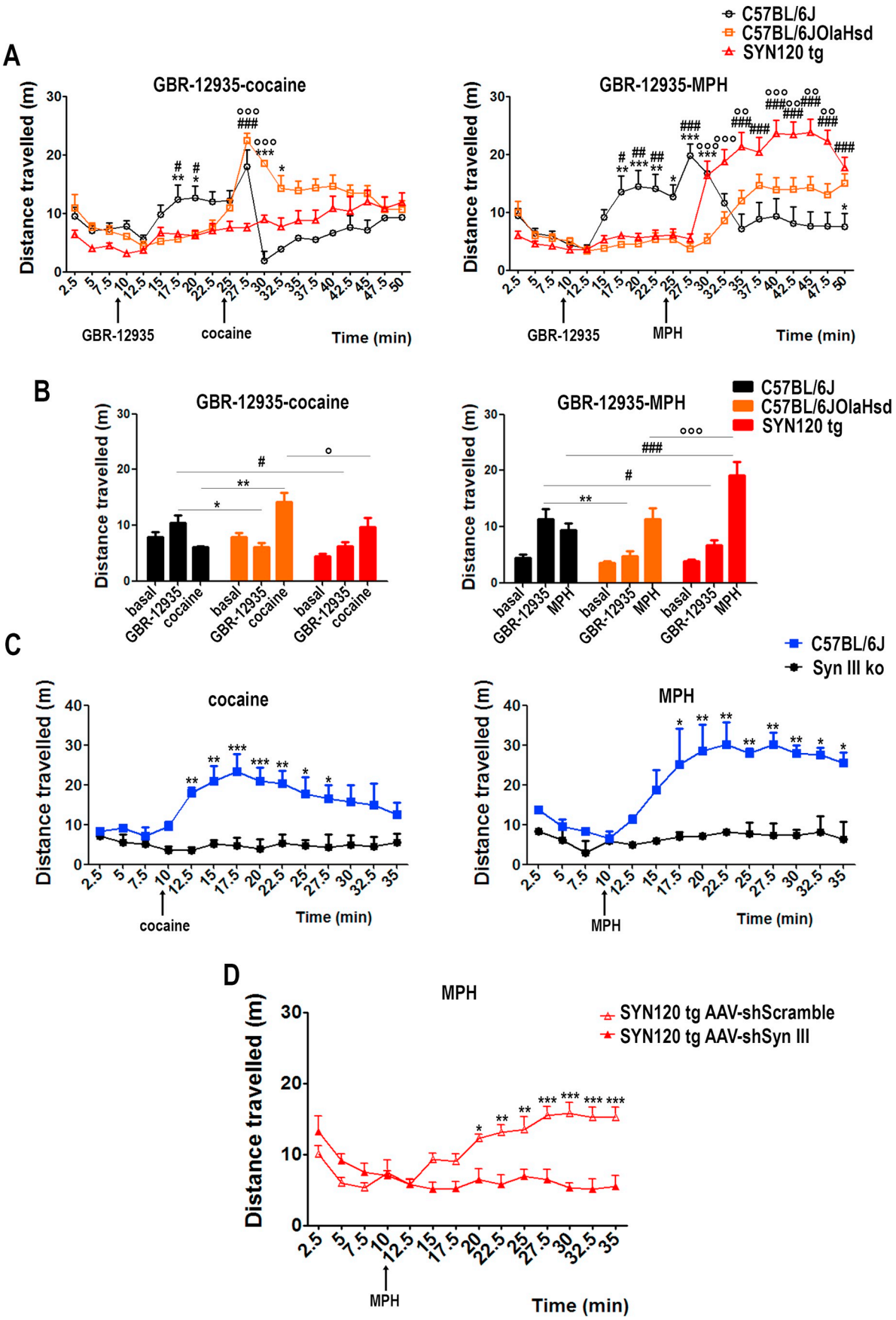

(caption on next page)

Fig. 5. Cocaine- and MPH-induced locomotor responses after GBR-12935 pretreatment in 12-month-old C57BL/6J, C57BL/6JOlaHsd and SYN120 tg mice.
A. Two-way ANOVA showed that the three mouse lines exhibited a differential locomotor response to the sequential administration of either GBR-12935 + cocaine (interaction: $F38,321 = 4.211$, $P < 0.0001$) or GBR-12935 + MPH (interaction: $F38,643 = 9.7$, $P < 0.0001$). After GBR-12935 administration we detected a decreased locomotor activity in C57BL/6JOlaHsd (* $P < 0.05$, ** $P < 0.01$, *** $P < 0.001$) and SYN120 tg mice (# $P < 0.05$, ## $P < 0.01$, ### $P < 0.001$) vs to C57BL/6J littermates. After cocaine stimulation C57BL/6J showed a peak of motility that was significantly higher than that observed in SYN120 tg (### $P < 0.001$) and C57BL/6JOlaHsd mice (***$P < 0.001$), but then rapidly dropped to basal levels. After cocaine administration the motility of C57BL/6JOlaHsd resulted significantly augmented when compared to SYN120 tg (°°° $P < 0.001$) and C57BL/6J mice (* $P < 0.05$ and *** $P < 0.001$). In C57BL/6J mice MPH induced a quick motility increase vs C57BL/6JOlaHsd (*** $P < 0.001$) and SYN120 tg mice (### $P < 0.001$), which rapidly dropped to basal values. MPH significantly enhanced the motility of SYN120 tg mice vs C57BL/6J (### $P < 0.001$) and C57BL/6JOlaHsd mice (°° $P < 0.01$ and °°° $P < 0.001$).
B. Statistically significant decrease of the locomotor activity of C57BL/6JOlaHsd (* $P < 0.05$, ** $P < 0.01$) and SYN120 tg mice (# $P < 0.05$) after GBR-12935 stimulation vs C57BL/6J littermates. Cocaine administration improved C57BL/6JOlaHsd mice motility vs C57BL/6J (** $P < 0.01$) and SYN120 tg animals (° $P < 0.05$). MPH-induced locomotor activity was instead enhanced in SYN120 tg mice vs C57BL/6J (### $P < 0.001$) and C57BL/6JOlaHsd mice (°°° $P < 0.001$).
C. Graphs are showing the locomotor response to either cocaine or MPH administration of 12-month-old C57BL/6J wt and Syn III ko mice. Two-way ANOVA showed a significant difference in the locomotor response of these mouse lines (cocaine: interaction: $F13,56 = 2.250$, $P < 0.05$ and MPH: interaction: $F13,40 = 2.103$, $P < 0.05$). Syn III ko mice did not respond to either cocaine or MPH administration (* $P < 0.05$, ** $P < 0.01$, *** $P < 0.001$ vs C57BL/6J).
D. Graphs are showing the locomotor response to MPH administration of 16-month-old SYN120 mice which were subjected to bilateral gene silencing of Syn III in the *substantia nigra*. Two-way ANOVA showed a significant difference (interaction: $F13,84 = 8.207$, $P < 0.0001$) in the locomotor response of these SYN120 tg mice who were injected with the AAV transducing Syn III shRNA (SYN120 tg AAV-shSyn III) or scramble-AAV (SYN120 tg AAV-shScramble). The injection of a sh-AAV producing Syn III gene silencing significantly reduced the MPH-induced locomotor activity in SYN120 tg mice, when compared to the littermates SYN120 tg animals injected with a scramble-AAV (* $P < 0.05$, ** $P < 0.01$, *** $P < 0.001$).

saline 0.9%) and analyzed. These mice showed a locomotor response that had similar basal conditions, supporting that the vehicle injection did not influence their motility (Supplementary Fig. 2B).

To further clarify the relevance of DAT blockade in cocaine- or MPH-induced locomotor activity, we analyzed the motility of 12-month-old mice after GBR-12935 administration, followed by either cocaine or MPH treatment (Fig. 5A,B). GBR-12935 pre-administration was used to induce DAT blockade, in order to ensure that the locomotor response observed after cocaine or MPH was independent of DAT inhibition. We found that SYN120 tg mice neither responded to GBR-12935, nor to the subsequent cocaine administration. C57BL/6J and C57BL/6JOlaHsd mice positively responded to GBR-12935 and showed a fast peak in motor activity 2.5 min after cocaine treatment, followed by different time-dependent attenuation (Fig. 5A). This phenomenon may be the result of a compensatory decrease of DA release deriving from an overstimulation of striatal D2 autoreceptors in response to the marked increase of extra-synaptic DA resulting from the additive effect of GBR-12935 and cocaine. The analysis of the total distance travelled in the three different experimental tranches (basal condition, GBR-12935 single administration, cocaine administration following GBR-12935) confirmed the above results (Fig. 5B).

When we analyzed the locomotor response to MPH administration after GBR-12935 (Fig. 5A), we found that SYN120 tg mice still exhibited an enhanced locomotion starting 5 min after MPH treatment. These findings suggest that the MPH-mediated stimulation of locomotor activity in SYN120 tg mice does not depend on DAT inhibition, which was achieved by GBR-12935-operated blockade, but rather on the pathological α-syn/Syn III interplay. In support of this, the motor response of C57BL/6J control mice resulted comparable to that observed after GBR-12935 plus cocaine injection, and C57BL/6JOlaHsd animals only showed a mild but not significant motility increase 10 min after MPH administration. The analysis of the total distance travelled in the different experimental tranches confirmed these results (Fig. 5B).

To evaluate the relevance of Syn III in the motor response to MPH, cocaine or vehicle administration, we performed the open field tests in 12-month-old Syn III ko and C57BL/6J mice (Fig. 5C, Supplementary Fig. 3A). We found that Syn III ko mice did not exhibit any improvements of motility after the administration of these drugs. This observation collimates with findings indicating that the ability of cocaine to enhance DA release is reduced in the absence of Syn III (Kile et al., 2010).

Finally, we probed whether the enhanced locomotor response to MPH administration observed in aged SYN120 tg mice could effectively be mediated by a cooperative action of α-syn and Syn III. To this purpose, 12-month-old SYN120 tg mice were subjected to AAV-mediated Syn III gene silencing and the locomotor response of these mice after an acute MPH challenge was evaluated at 16 months of age (Fig. 5D). Quantification of Syn III immunolabeling in the *substantia nigra* of mice showed a statistically significant reduction of Syn III-positive area in the animals which were injected with the AAV transducing the Syn III shRNA (Supplementary Fig. 3B,C). Remarkably, the animals subjected to Syn III gene silencing lost the capability to respond to MPH administration, while those injected with the AAV transducing scramble shRNA sequences could still respond to the drug. This observation confirms that Syn III is implicated in MPH action. In light of our previous findings showing that 12 and 16-month-old C57BL/6JOlaHsd mice, that express elevated Syn III levels in the absence of α-syn, did not exhibit the paradoxical increase in locomotion observed in SYN120 tg mice, the latter results further suggest that MPH-mediated stimulation of locomotor activity may be co-orchestrated by α-syn and Syn III pathological cooperation.

3.4. MPH stimulates the interaction between Syn III and fl or (1–120) human α-syn

To better understand how cocaine, MPH (d-*threo*) or GBR-12935 could affect the interplay between α-syn and Syn III, we evaluated whether an acute 15 min treatment with these compounds could affect the interaction between either fl or (1–120) α-syn and Syn III by using acceptor photobleaching FRET (Fig. 6A), in a cell culture system reproducing α-syn/Syn III inclusion formation. Acceptor photobleaching FRET microscopy allows an accurate evaluation of protein-protein interaction through the measurement of FRET efficiency. This parameter is indicative of the increase of donor fluorescence after complete photobleaching of the acceptor fluorescence, within a FRET pair of fluorophores (where the emission wavelength of a donor falls within the excitation wavelength of an acceptor). Since FRET efficiency is detectable only when the two fluorophores are sufficiently close to ensure that their linked proteins are interacting, the molecular proximity of these latter results strictly dependent on this parameter (Bajar et al., 2016; Ishikawa-Ankerhold et al., 2012).

In particular, we used SK-N-SH cells overexpressing GFP-tagged Syn III (Syn III-GFP) together with either RFP-tagged fl α-syn (fl*α-syn*-RFP) or RFP-tagged (1–120) α-syn-RFP (120α-syn-RFP) that, in line with previous findings (Fares et al., 2016), can lead to the formation of insoluble intracellular inclusions composed of either fl or C-terminally truncated α-syn. Negative controls were also performed to confirm the specificity of FRET signal. In particular, in order to assess that GFP signal recovery was directly dependent on RFP bleaching, FRET efficiency was measured on cells with the sole RFP-α-syn transfection. Results (not shown) supported the absence of photobleaching recovery in single RFP-α-syn-transfected cells.

By confocal microscopy we observed that SK-N-SH cells transducing

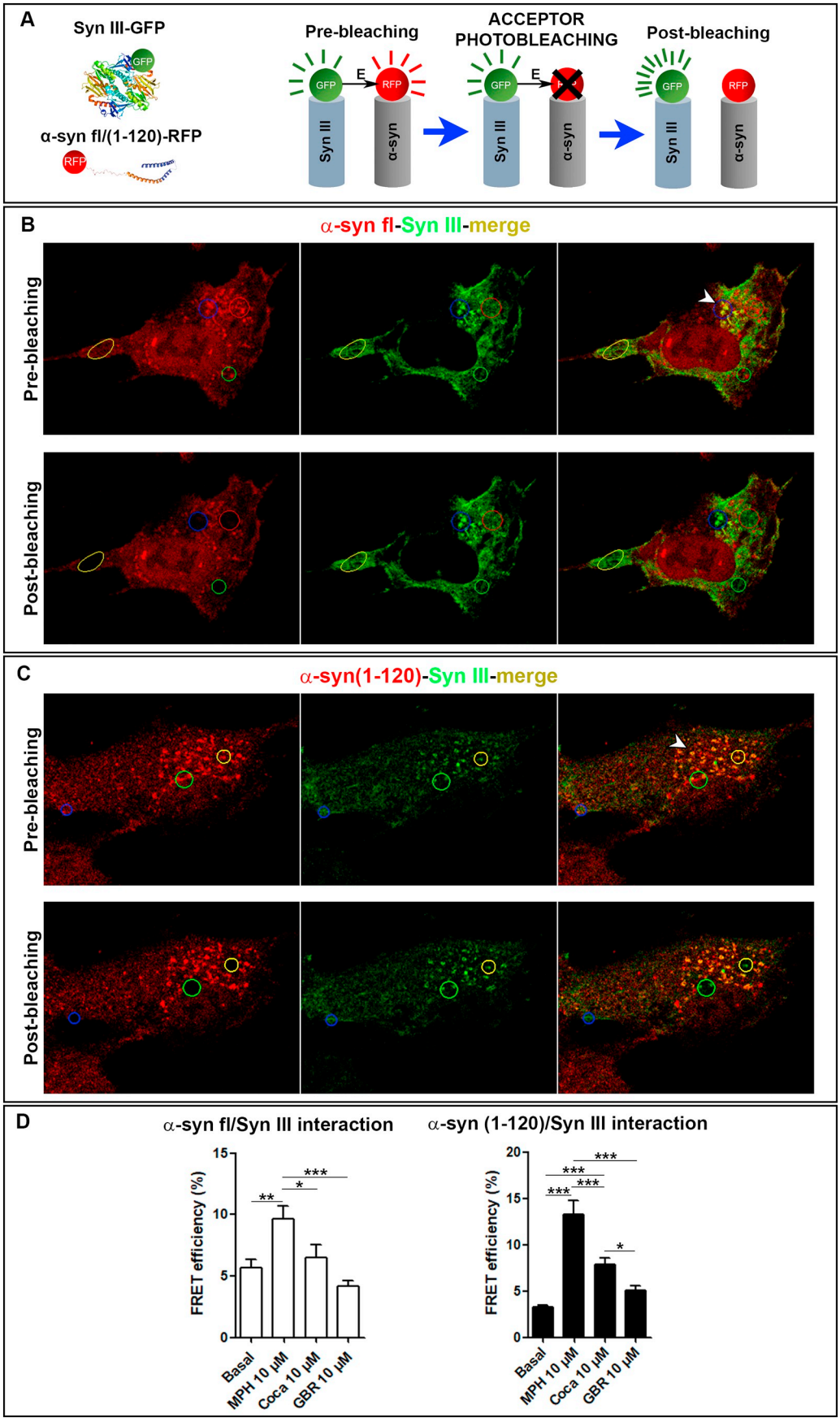

Fig. 6. FRET-based analysis of fl α-syn/Syn III and (1–120) α-syn/Syn III interaction in SH-N-SK cells.

A. Schematic representation of the acceptor photobleaching FRET experimental set up used to investigate the interaction between Syn III-GFP with either fl*α-syn*-RFP or 120α-syn-RFP. Before the bleaching (Pre-bleaching) energy is transferred from the donor to the acceptor fluorophore, after the bleaching of the acceptor (Post-bleaching) the increase in donor fluorescence is measured and the FRET efficiency is dependent on the molecular proximity.

B. Representative images of SK-N-SH transducing both flα-syn-RFP and Syn III-GFP before (upper panels) and after (lower panels) RFP photobleaching.

C. Representative images of SK-N-SH transducing both 120α-syn-RFP and Syn III-GFP before (upper panels) and after (lower panels) the RFP photobleaching.

D. Histograms are showing the FRET efficiency of flα-syn-RFP with Syn III-GFP and of 120α-syn-RFP with Syn III-GFP in basal condition or registered 15 min after MPH, cocaine or GBR-12935 administration (* $P < 0.05$; ** $P < 0.01$, *** $P < 0.001$, One-way ANOVA + Newman-Keuls post-comparison test).

either flα-syn-RFP or 120α-syn-RFP and Syn III-GFP exhibited intracellular round-shaped inclusions which resulted positive for both RFP and GFP (Fig. 6B,C), thus supporting that they contained either both fl α-syn and Syn III or both (1–120) α-syn and Syn III. By FRET analysis, we then found that the fl α-syn and Syn III or (1–120) α-syn and Syn III co-transfected cells treated with vehicle for 15 min showed a basal % FRET efficiency of 5.7 ± 0.62 and 3.27 ± 0.22, respectively (Fig. 6D). Notably, 15 min of MPH treatment significantly increased the interaction between fl α-syn and Syn III when compared to the cells in basal condition or to those treated with cocaine or GBR-12935 (Fig. 6D). Remarkably, MPH resulted even more efficient in improving the interaction between Syn III and (1–120) α-syn vs the respective vehicle treated controls or to the cells that were treated with cocaine or GBR-12935 (Fig. 6D). Cocaine mildly improved the interaction between Syn III and (1–120) α-syn when compared to the vehicle-treated cells, although with an efficacy that was almost the half of MPH, but had no effect on Syn III /fl α-syn binding. Finally, GBR-12935 did not affect the interaction between Syn III and either fl or (1–120) α-syn (Fig. 6D).

4. Discussion

The results of this study support that in the presence of α-syn/Syn III co-aggregates, specific α-syn conformational variants can contribute to foster a Syn III-dependent locomotor response to MPH. In particular, our FRET studies in SK-N-SH cells containing α-syn and Syn III-positive inclusions, support that MPH promotes the interaction between fl or (1–120) α-syn and Syn III, suggesting that the establishment of a functional binding between α-syn and Syn III is necessary to mediate the stimulatory action of this drug.

As observed in the *post mortem* brains of PD patients (Longhena et al., 2018) and in an AAV-based mouse model of PD (Faustini et al., 2018), we found that Syn III forms fibrillary co-aggregates with C-terminally-truncated α-syn also in the brain of SYN120 tg mice. When we analyzed the levels of Syn III in the *striatum* of C57BL/6J, C57BL/6JOlaHsd α-syn null and SYN120 tg mice along aging, we found that it was highly expressed in the brain of mice lacking α-syn, especially at 8 and 12 months of age, but not in C57BL/6J wt littermates. Surprisingly, at 3 and 8 months of age, the levels of Syn III in the *striatum* of SYN120 tg mice were lower than in α-syn null littermates, but then raised at later time points. In line with our previous findings supporting a negative modulatory action of α-syn on Syn III expression (Zaltieri et al., 2015), this observation may indicate that the production of C-terminally truncated α-syn on the C57BL/6JOlaHsd background results in a compensatory down-regulation of Syn III in young SYN120 tg mice. This is then lost along aging when most of α-syn is aggregated and the levels of Syn III are increased.

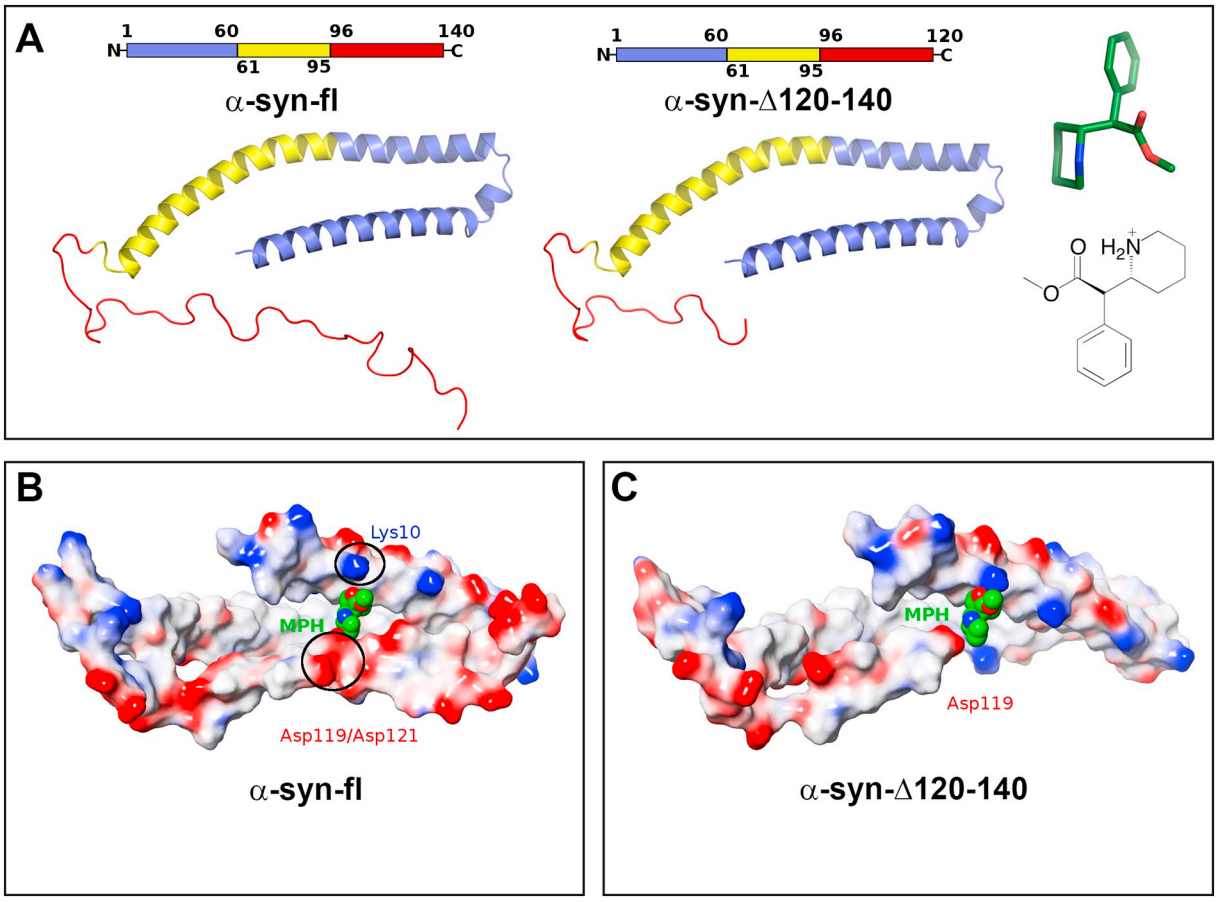

Fig. 7. *In-silico* simulation of MPH and fl or (1–120) α-syn interaction.
A. Cartoon representation of α-syn fl (1–140) and α-syn-Δ120–140 (1–120). The N-Terminal domain (residues 1–60), the central hydrophobic region (residues 61–95) and the C-terminal domain (residues 96–140/120) are colored in blue, yellow and red, respectively. Both 3-D (green sticks) and 2-D structure of *d-threo*-MPH are depicted.
B. MPH (as green, red and blues spheres) in complex with fl α-syn (as surface color coded accordingly to residue charges, where red indicates negatively charged residues, blue positively charged residues and white hydrophobic residues). The Lys110 and Asp119–120 are highlighted in black circles. C. MPH (as green, red and blues spheres) in complex with α-syn-Δ120–140 (as surface color coded accordingly to residue charges, where red indicates negatively charged residues, blue positively charged residues and white hydrophobic residues). (For interpretation of the references to color in this figure legend, the reader is referred to the web version of this article.)

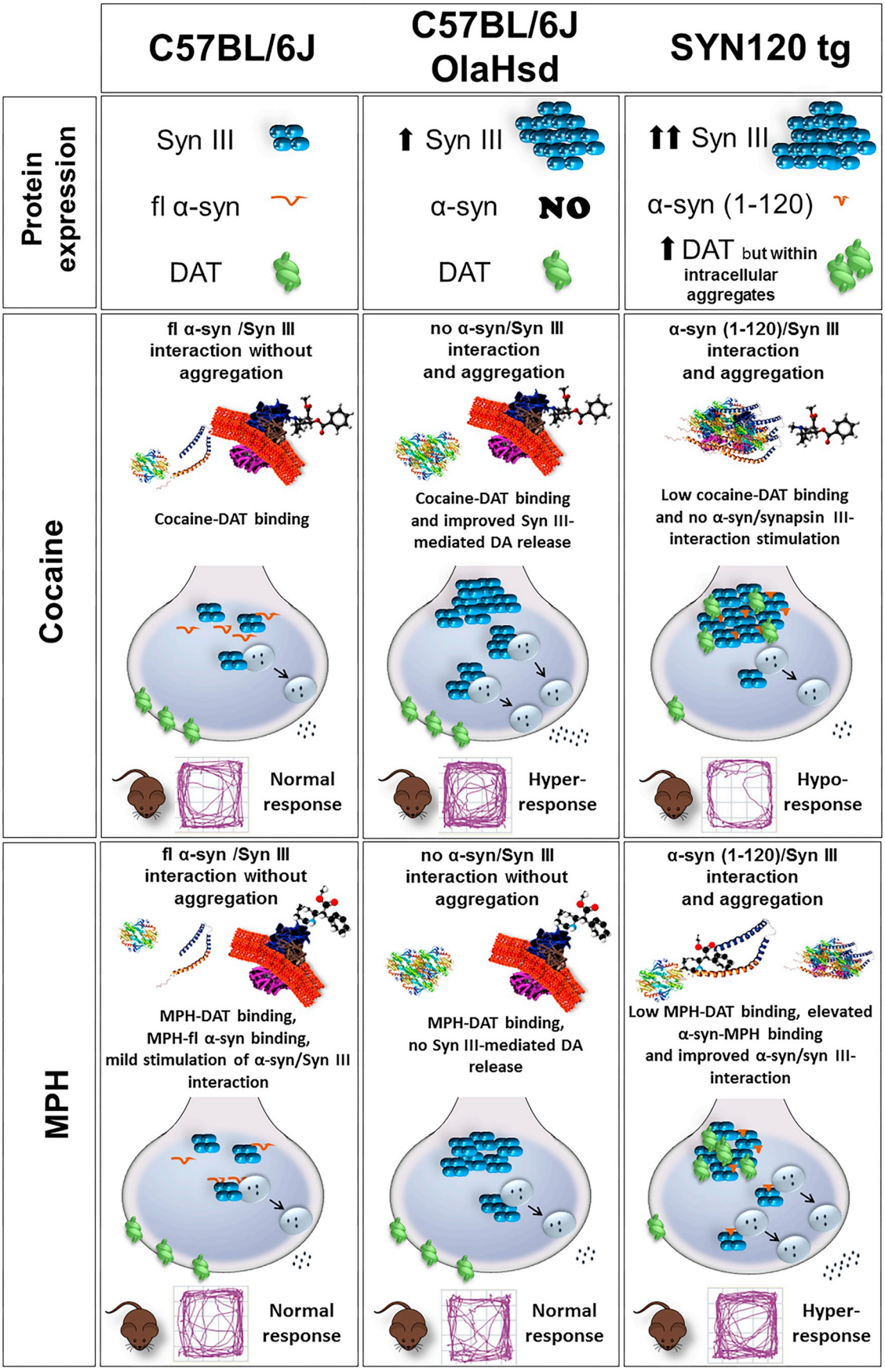

(caption on next page)

Fig. 8. Schematic representation of the mechanisms and behavioral readout of the differential effect of cocaine and MPH in C57BL/6J, C57BL/6JOlaHsd and SYN120 tg mice at 12 months of age.
Syn III and α-syn are both involved in mediating the motor response to cocaine and MPH. Cocaine stimulated the motility of α-syn null mice, which showed elevated Syn III expression and DAT levels comparable to C57BL/6J mice, supporting that part of the cocaine-stimulated response of these mice is dependent on Syn III. MPH effect can be positively fostered in the presence of α-syn and Syn III co-aggregates, in particular when the levels of these proteins are markedly elevated. MPH stimulates α-syn/Syn III interaction in cells showing α-syn/Syn III co-aggregates likely by stabilizing α-syn in a conformation with low aggregation propensity.

Quantitative PCR studies in the *substantia nigra* of mice at 3 and 12 months of age showed that Syn III mRNA expression in this area fairly recapitulated the changes in protein levels observed in the *striatum*, thus further confirming the existence of a reciprocal regulatory interplay between the expression of α-syn and syn III.

By analyzing the motility of C57BL/6J, C57BL/6JOlaHsd α-syn null and SYN120 tg mice after the acute cocaine, MPH or GBR-12935 administration, although these are all known to act as DAT blockers, we found peculiar differences in the locomotor response of the three mouse lines. In particular, only C57BL/6J mice positively and similarly responded to cocaine, MPH and GBR-12935, while α-syn null and SYN120 tg mice were almost insensitive to GBR-12935 administration. This notwithstanding, they exhibited a differential age-related motility profile after the i.p. injection of cocaine or MPH. While the motility of SYN120 tg mice was almost unaffected by cocaine administration at all the time points analyzed, C57BL/6JOlaHsd mice exhibited a marked response at 8 and 12 months of age, when the levels of Syn III were higher, but those of DAT protein were comparable to C57BL/6J mice. This effect was partially attenuated by the pre-administration of GBR-12935, supporting that only part of the cocaine-stimulated response of α-syn null mice is dependent on DAT inhibition. However, these animals lost their capability to respond to cocaine at 16 months of age, probably because the differences in Syn III expression levels, when compared to C57BL/6J mice, become milder at this time point.

We previously showed that cocaine treatment prevents the formation of α-syn-positive inclusions in cells exposed to glucose deprivation, an insult stimulating α-syn aggregation (Bellucci et al., 2008). Cocaine can bind the α-syn N-terminus, acts as an α-syn modulator and induces a conformational shift of the protein (Jakova and Lee, 2017; Kakish et al., 2015). Moreover, cocaine abuse increases α-syn in dopaminergic neurons or in the *striatum* (Mash et al., 2003; Qin et al., 2005) and α-syn has been found to be critical for cocaine preference (Trubetckaia et al., 2019). The present results support that elevated Syn III levels are crucial for allowing cocaine response in the absence of α-syn and that cocaine is not able to affect the motor response of mice when α-syn is aggregated. This suggests that 1) cocaine-stimulated locomotor response is partly dependent on Syn III and 2) α-syn conformational state is critical for enabling cocaine binding and the consequent motor effects.

By analyzing the locomotor activity of mice in response to MPH administration, we found that C57BL/6J and C57BL/6JOlaHsd mice exhibited similar responses at 3, 8 and 12 months of age. At 3 and 8 months of age, also the locomotor response of SYN120 tg mice following MPH administration was comparable to that observed in C57BL/6J and C57BL/6JOlaHsd mice. Though unexpectedly, SYN120 tg mice exhibited an over-increase in the locomotor response, which resulted markedly enhanced with respect to that of the other mouse lines, at 12 and 16 months of age. Strikingly, this over-response was not perturbed by GBR-12935-mediated DAT inhibition and was lost in mice subjected to Syn III gene silencing. This suggests that the increased locomotor response observed in SYN120 tg mice following MPH treatment is not dependent on DAT blockade, but is rather crucially mediated by Syn III.

We also observed that Syn III ko mice did not respond to cocaine or MPH administration, although they did not display differences in DAT striatal levels (Faustini et al., 2018). This is fully in line with previous findings showing that cocaine reduces striatal DA release in these mice (Kile et al., 2010) and sustains that cocaine and MPH effect is dependent on the presence of Syn III. However, the Syn III-mediated locomotor activity can be alternatively influenced in the absence or in the presence of different α-syn conformational variants.

The observation that aged SYN120 tg mice, which show elevated α-syn aggregation, acquire the ability to respond to MPH treatment, is reminiscent of the fact that MPH efficiently counteracts freezing of gait and hypokinesia in advanced PD patients (Delval et al., 2015; Devos et al., 2007; Moreau et al., 2012; Nikolai Gil et al., 2018; Pollak et al., 2007). This effect does not rely on the increase in attentional performance (Delval et al., 2015) and, although it can enhance L-DOPA efficacy (Camicioli et al., 2001), it does not necessarily require exogenous L-DOPA (Pollak et al., 2007). It has been also observed that MPH can redistribute DA vesicle pools (Sandoval et al., 2003). In light of our results, we may speculate that the MPH-associated trafficking of synaptic vesicles in dopaminergic neurons could be mediated by α-syn/Syn III interplay, as these proteins can both control synaptic vesicle pools (Burre, 2015; Cesca et al., 2010). MPH has demonstrated therapeutic efficacy in ADHD (Huss et al., 2017), a neurodevelopmental disorder whose onset has been found to positively correlate with the 631C > G Syn III polymorphism (Kenar et al., 2013), which can contribute to the efficacy of MPH itself (Basay et al., 2016). Our group has also shown that Syn III is a crucial mediator of early neuronal development, migration and orientation (Perlini et al., 2015; Piccini et al., 2015), findings that further support that Syn III polymorphisms may significantly contribute to the neurodevelopmental change underlying ADHD. Interestingly, ADHD patients manifest a psychostimulant-medication independent predisposition to develop disorders of the basal ganglia, including PD and LB dementia (Curtin et al., 2018; Golimstok et al., 2011). Moreover, a recent study supports that the rs356219 genotype in SNCA may affect α-syn function and contribute to the etiology of ADHD (Gerlach et al., 2019). These findings corroborate the existence of a crucial link between Syn III and α-syn in the pathophysiology of LB disorders and possibly of ADHD.

Cocaine and MPH have been found to bind α-syn. In particular, the former binds the N-terminus of α-syn and prompts the formation of more compact protein conformation, while the latter promotes loop-like α-syn folding through a contemporaneous strong N-terminal and weak C-terminal interaction (Kakish et al., 2015). Cocaine and MPH can increase or decrease DA neurotransmission by blocking reuptake and reducing exocytotic release, respectively (Federici et al., 2014). Moreover, while cocaine can stimulate Syn III-dependent DA release independently of Calcium concentrations (Kile et al., 2010), MPH can influence α-syn-mediated DA overflow and presynaptic compartmentalization, but its effect on DA reuptake is independent of α-syn (Chadchankar et al., 2012). Our results support that cocaine action is not significantly influenced by the pathological α-syn/Syn III interplay, which however actively contributes to the effect of MPH.

It has been shown that, in pathological conditions, α-syn can form metastable cytotoxic oligomers which give raise to the formation of the insoluble fibrils composing LB (Longhena et al., 2019). In such cases, following a basic aggregation mechanism (Chiti and Dobson, 2006), it has been hypothesized that the central hydrophobic core (residue 61–95) adopts in-register β-sheets conformations, promoting fibril formation (Tuttle et al., 2016). Interestingly, by concurrently binding both the N- and C-termini of α-syn (but not the central region), MPH interacts with α-syn in such a way that stabilizes the protein in a conformation less prone to aggregate and can thus be considered neuroprotective (Kakish et al., 2015). The NMR structure of α-syn previously

reported in Rao et al., (2010) showed the presence of 2KKW sequence that can be identified as a potential source of interesting α-syn conformations suitable for such task. Indeed, by combining NMR and spin labelling/electron paramagnetic resonance (EPR), Rao and co-workers reported an ensemble of 34 α-syn structures exhibiting partially folded conformations upon micelle binding (Rao et al., 2010). In one of these conformations, by showing an N-terminal domain folded into a classical α-helix secondary element in close proximity to the unfolded C-terminal domain and the central core adopting α-helix structure, α-syn results less prone to generate fibrillary aggregates (Kakish et al., 2015; Rao et al., 2010). In the attempt to confirm the heuristic model for α-syn in complex with MPH by Kakish and co-authors (Kakish et al., 2015), we identified one α-syn conformation able to interact with MPH within those reported by Rao and co-authors (Fig. 7A). Docking studies of MPH in its *d-threo* configuration and this particular fl α-syn conformation confirmed that MPH interacts with the α-helix secondary element-folded N-terminal domain of α-syn through the positively charged Lys10 residue (Fig. 7B). Concomitantly, it plunges the positively charged nitrogen atom into a region of the proximal unfolded C-terminal domain enriched in negatively charged residues and defined by Asp119 and Asp121 residues, while the central core is stabilized into an α-helix (Fig. 7B). This *in silico* model sounds also in agreement with above described data showing that MPH is effective on SYN120 tg mice, since Asp119 is conserved in the (1–120) α-syn construct (Fig. 7C), thus supporting the reliability of the generated complexes.

These observations provide putative structural details underlying the protective effect of MPH on α-syn/Syn III neuropathology. In particular, they support that MPH stabilizes α-syn into a conformation not suitable to fibrillary aggregation, which rather displays improved capacity to establish a functional interaction with Syn III, that in turn results in the observed Syn III-dependent locomotor activity. Interestingly, this conformation is stabilized by micelle binding (Rao et al., 2010), suggesting that lipids, or more probably synaptic vesicle proximity, may promote its formation. Notably, α-syn aggregation can cluster and disorganize synaptic vesicles (Faustini et al., 2018; Wang et al., 2014). This evidence, when coupled to recent findings showing that LB are constituted by a lipid crowded environment which contains dispersed protein filaments (Shahmoradian et al., 2019), supports that synaptic vesicles and organelles may be entrapped by α-syn/Syn III fibrillary aggregates during LB formation. It may thus be feasible that along with α-syn fibril deposition, different α-syn conformational variants with diverse lipid binding affinity and function may be easily generated. The Syn III-dependent MPH effect, likely mediated by an N-terminal and central region α-helical α-syn conformation resulting from lipid interaction, occurs only in aged SYN120 tg mice and seems to be fully in line with a progressive lipid crowding model of LB. This notwithstanding, due to the dynamic nature of α-syn, we cannot firmly exclude that MPH could also stabilize different conformation/s with respect of that analyzed in this study. It may be also feasible that specific post-translational modifications of α-syn may be relevant for MPH action in SYN120 tg mice.

5. Conclusions

Collectively, our results support that Syn III and α-syn are both involved in mediating the motor response to cocaine and MPH (Fig. 8). Furthermore, they unveil that MPH effect can be positively fostered in the presence of α-syn and Syn III co-aggregates, in particular when the levels of these proteins are markedly elevated. Finally, we also found that MPH stimulates α-syn/Syn III interaction in cells showing α-syn/Syn III co-aggregates and provided a model supporting that this drug stabilizes α-syn in a conformation with low aggregation propensity. When seen in the light of clinical studies supporting the efficacy of MPH in counteracting freezing of gait in advanced PD, our findings hint that α-syn/Syn III pathological coaction could be the mediator of this effect. This supports that drugs modulating α-syn/Syn III interplay may constitute valid therapeutic options for treating this neurodegenerative disorder. Not least, they hold significant implications also in the field of ADHD.

Supplementary data to this article can be found online at https://doi.org/10.1016/j.nbd.2020.104789.

Funding

This work was supported by Fondazione Cariplo (2014-0769), the University of Brescia (BIOMANE), the Italian Ministry of Instruction, University and Research, Programma Nazionale per la Ricerca (MIUR, PNR) 2015–2020 Personalized Medicine for Innovative Strategies in Neuro-Psychiatric and Vascular Diseases (PerMedNet), the Michael J. Fox Foundation for Parkinson's Research, NY, USA (grant ID #10742.01).

Declaration of Competing Interest

The authors declare no conflict of interest.

References

Adamczyk, A., et al., 2006. Alpha-synuclein and its neurotoxic fragment inhibit dopamine uptake into rat striatal synaptosomes. Relationship to nitric oxide. Neurochem. Int. 49, 407–412.
Al-Wandi, A., et al., 2010. Absence of alpha-synuclein affects dopamine metabolism and synaptic markers in the striatum of aging mice. Neurobiol. Aging 31, 796–804.
Bajar, B.T., et al., 2016. A guide to fluorescent protein FRET pairs. Sensors (Basel). 16.
Basay, O., et al., 2016. The impact of synapsin III gene on the neurometabolite level alterations after single-dose methylphenidate in attention-deficit hyperactivity disorder patients. Neuropsychiatr. Dis. Treat. 12, 1141–1149.
Bellucci, A., et al., 2008. Alpha-synuclein aggregation and cell death triggered by energy deprivation and dopamine overload are counteracted by D2/D3 receptor activation. J. Neurochem. 106, 560–577.
Bellucci, A., et al., 2011. Redistribution of DAT/alpha-synuclein complexes visualized by "in situ" proximity ligation assay in transgenic mice modelling early Parkinson's disease. PLoS One 6, e27959.
Bellucci, A., et al., 2014. The "in situ" proximity ligation assay to probe protein-protein interactions in intact tissues. Methods Mol. Biol. 1174, 397–405.
Bellucci, A., et al., 2016. Review: Parkinson's disease: from synaptic loss to connectome dysfunction. Neuropathol. Appl. Neurobiol. 42, 77–94.
Bogen, I.L., et al., 2006. Absence of synapsin I and II is accompanied by decreases in vesicular transport of specific neurotransmitters. J. Neurochem. 96, 1458–1466.
Burre, J., 2015. The synaptic function of alpha-Synuclein. J. Parkinsons Dis. 5, 699–713.
Camicioli, R., et al., 2001. Methylphenidate increases the motor effects of L-Dopa in Parkinson's disease: a pilot study. Clin. Neuropharmacol. 24, 208–213.
Cesca, F., et al., 2010. The synapsins: key actors of synapse function and plasticity. Prog. Neurobiol. 91, 313–348.
Chadchankar, H., et al., 2012. Methylphenidate modifies overflow and presynaptic compartmentalization of dopamine via an alpha-synuclein-dependent mechanism. J. Pharmacol. Exp. Ther. 341, 484–492.
Chiti, F., Dobson, C.M., 2006. Protein misfolding, functional amyloid, and human disease. Annu. Rev. Biochem. 75, 333–366.
Chu, Y., et al., 2019. Intrastriatal alpha-synuclein fibrils in monkeys: spreading, imaging and neuropathological changes. Brain. 142, 3565–3579.
Connor-Robson, N., et al., 2016. Combinational losses of synucleins reveal their differential requirements for compensating age-dependent alterations in motor behavior and dopamine metabolism. Neurobiol. Aging 46, 107–112.
Crowther, R.A., et al., 1998. Synthetic filaments assembled from C-terminally truncated alpha-synuclein. FEBS Lett. 436, 309–312.
Curtin, K., et al., 2018. Increased risk of diseases of the basal ganglia and cerebellum in patients with a history of attention-deficit/hyperactivity disorder. Neuropsychopharmacology. 43, 2548–2555.
Delval, A., et al., 2015. Gait and attentional performance in freezers under methylphenidate. Gait Posture 41, 384–388.
Devos, D., et al., 2007. Improvement of gait by chronic, high doses of methylphenidate in patients with advanced Parkinson's disease. J. Neurol. Neurosurg. Psychiatry 78, 470–475.
Fares, M.B., et al., 2016. Induction of de novo alpha-synuclein fibrillization in a neuronal model for Parkinson's disease. Proc. Natl. Acad. Sci. U. S. A. 113, E912–E921.
Faustini, G., et al., 2018. Synapsin III deficiency hampers alpha-synuclein aggregation, striatal synaptic damage and nigral cell loss in an AAV-based mouse model of Parkinson's disease. Acta Neuropathol. 136, 621–639.
Federici, M., et al., 2014. Paradoxical abatement of striatal dopaminergic transmission by cocaine and methylphenidate. J. Biol. Chem. 289, 264–274.
Fountaine, T.M., Wade-Martins, R., 2007. RNA interference-mediated knockdown of alpha-synuclein protects human dopaminergic neuroblastoma cells from MPP(+) toxicity and reduces dopamine transport. J. Neurosci. Res. 85, 351–363.
Garcia-Reitbock, P., et al., 2010. SNARE protein redistribution and synaptic failure in a

transgenic mouse model of Parkinson's disease. Brain. 133, 2032–2044.
Gerlach, M., et al., 2019. Family-based association study on functional alpha-synuclein polymorphisms in attention-deficit/hyperactivity disorder. Atten Defic Hyperact Disord. 11, 107–111.
Golimstok, A., et al., 2011. Previous adult attention-deficit and hyperactivity disorder symptoms and risk of dementia with Lewy bodies: a case-control study. Eur. J. Neurol. 18, 78–84.
Hosaka, M., Sudhof, T.C., 1998. Synapsin III, a novel synapsin with an unusual regulation by Ca2+. J. Biol. Chem. 273, 13371–13374.
Huss, M., et al., 2017. Methylphenidate dose optimization for ADHD treatment: review of safety, efficacy, and clinical necessity. Neuropsychiatr. Dis. Treat. 13, 1741–1751.
Ishikawa-Ankerhold, H.C., et al., 2012. Advanced fluorescence microscopy techniques–FRAP, FLIP, FLAP, FRET and FLIM. Molecules. 17, 4047–4132.
Jakova, E., Lee, J.S., 2017. Behavior of alpha-synuclein-drug complexes during nanopore analysis with a superimposed AC field. Electrophoresis. 38, 350–360.
Kakish, J., et al., 2015. Drugs that bind to alpha-Synuclein: Neuroprotective or Neurotoxic? ACS Chem. Neurosci. 6, 1930–1940.
Kenar, A.N., et al., 2013. Association of synapsin III gene with adult attention deficit hyperactivity disorder. DNA Cell Biol. 32, 430–434.
Kile, B.M., et al., 2010. Synapsins differentially control dopamine and serotonin release. J. Neurosci. 30, 9762–9770.
Lee, F.J., et al., 2001. Direct binding and functional coupling of alpha-synuclein to the dopamine transporters accelerate dopamine-induced apoptosis. FASEB J. 15, 916–926.
Longhena, F., et al., 2018. Synapsin III is a key component of alpha-synuclein fibrils in Lewy bodies of PD brains. Brain Pathol. 28, 875–888.
Longhena, F., et al., 2019. Living in promiscuity: the multiple Partners of Alpha-Synuclein at the synapse in physiology and pathology. Int. J. Mol. Sci. 20.
Mash, D.C., et al., 2003. Cocaine abusers have an overexpression of alpha-synuclein in dopamine neurons. J. Neurosci. 23, 2564–2571.
Mattick, J.S., 2004. RNA regulation: a new genetics? Nat. Rev. Genet. 5, 316–323.
Moreau, C., et al., 2012. Methylphenidate for gait hypokinesia and freezing in patients with Parkinson's disease undergoing subthalamic stimulation: a multicentre, parallel, randomised, placebo-controlled trial. Lancet Neurol. 11, 589–596.
Nikolai Gil, D., Reyes, M.A.C.B., Athena Kate, D., Jamora, A.R.D.G., 2018. High dose methylphenidate in the treatment of freezing of gait in advanced Parkinson's disease. Basal Ganglia 8–13.
Oaks, A.W., Marsh-Armstrong, N., Jones, J.M., Credle, J.J., Sidhu, A., 2013. Synucleins Antagonize Endoplasmic Reticulum Function to Modulate Dopamine Transporter Trafficking. PLoS One 8, e70872. https://doi.org/10.1371/journal.pone.0070872.
Paxinos, G.F., 2012. Paxinos and Franklin's the Mouse Brain in Stereotaxic Coordinates 4th Edition ed. ed. A. Press.
Perlini, L.E., et al., 2015. Synapsin III acts downstream of semaphorin 3A/CDK5 signaling to regulate radial migration and orientation of pyramidal neurons in vivo. Cell Rep. 11, 234–248.
Piccini, A., et al., 2015. Phosphorylation by PKA and Cdk5 mediates the early effects of Synapsin III in neuronal morphological maturation. J. Neurosci. 35, 13148–13159.
Pollak, L., et al., 2007. Low dose methylphenidate improves freezing in advanced Parkinson's disease during off-state. J. Neural Transm. Suppl. 145–148.
Prasad, K., et al., 2012. Critical role of truncated alpha-synuclein and aggregates in Parkinson's disease and incidental Lewy body disease. Brain Pathol. 22, 811–825.
Qin, Y., et al., 2005. Cocaine abuse elevates alpha-synuclein and dopamine transporter levels in the human striatum. Neuroreport. 16, 1489–1493.
Rao, J.N., et al., 2010. A combinatorial NMR and EPR approach for evaluating the structural ensemble of partially folded proteins. J. Am. Chem. Soc. 132, 8657–8668.
Sandoval, V., et al., 2003. Methylphenidate alters vesicular monoamine transport and prevents methamphetamine-induced dopaminergic deficits. J. Pharmacol. Exp. Ther. 304, 1181–1187.
Shahmoradian, S.H., et al., 2019. Lewy pathology in Parkinson's disease consists of crowded organelles and lipid membranes. Nat. Neurosci. 22, 1099–1109.
Spillantini, M.G., et al., 1997. Alpha-synuclein in Lewy bodies. Nature. 388, 839–840.
Tang, Y., et al., 2013. Fast vesicle transport is required for the slow axonal transport of synapsin. J. Neurosci. 33, 15362–15375.
Tofaris, G.K., et al., 2006. Pathological changes in dopaminergic nerve cells of the substantia nigra and olfactory bulb in mice transgenic for truncated human alpha-synuclein(1−120): implications for Lewy body disorders. J. Neurosci. 26, 3942–3950.
Trubetckaia, O., et al., 2019. Alpha-synuclein is strategically positioned for afferent modulation of midbrain dopamine neurons and is essential for cocaine preference. Commun Biol. 2, 418.
Tuttle, M.D., et al., 2016. Solid-state NMR structure of a pathogenic fibril of full-length human alpha-synuclein. Nat. Struct. Mol. Biol. 23, 409–415.
Venton, B.J., et al., 2006. Cocaine increases dopamine release by mobilization of a synapsin-dependent reserve pool. J. Neurosci. 26, 3206–3209.
Wang, L., et al., 2014. Alpha-synuclein multimers cluster synaptic vesicles and attenuate recycling. Curr. Biol. 24, 2319–2326.
Wersinger, C., Sidhu, A., 2003. Attenuation of dopamine transporter activity by alpha-synuclein. Neurosci. Lett. 340, 189–192.
Wersinger, C., Sidhu, A., 2005. Disruption of the interaction of alpha-synuclein with microtubules enhances cell surface recruitment of the dopamine transporter. Biochemistry. 44, 13612–13624.
Zaltieri, M., et al., 2015. Alpha-synuclein and synapsin III cooperatively regulate synaptic function in dopamine neurons. J. Cell Sci. 128, 2231–2243.